

## Phytochemical and Biological Activity Studies of The Leaves of *Garcinia hombroniana* Pierre

Nadia Rosli<sup>1</sup>, Melati Khairuddean<sup>1\*</sup> and Zuhair Jamain<sup>2</sup>

<sup>1</sup>School of Chemical Sciences, Universiti Sains Malaysia (USM), 11800 Penang, Malaysia

<sup>2</sup>Faculty of Science and Natural Resources, Universiti Malaysia Sabah (UMS),

88400 Kota Kinabalu, Sabah, Malaysia

\*Corresponding author (e-mail: melati@usm.my)

*Garcinia* is the biggest genus in the family of Clusiaceae (Guttiferae). *Garcinia* has gained a wide interest of researchers due to the remedial qualities and it has been used in traditional therapies and medicine. Our research work focused on the phytochemical investigation and biological activity studies of the leaves of *Garcinia hombroniana*. The phytochemical investigation of the chloroform extract of *G. hombroniana* had led to the isolation of ten known compounds, identified as friedelin (CP-1), stigmasterol (CP-2), taraxerol (CP-3), garihombromane D (CP-4), lupeol (CP-5), betulin (CP-6), betulinic acid (CP-7), stigmasterol glucoside (CP-8), 4-hydroxybenzoic acid (CP-9), and palmitic acid (CP-10). The isolated compounds recovered from column chromatography were purified using recrystallization technique. Structure elucidation of pure compounds was determined using Fourier Transform Infrared (FTIR), Nuclear Magnetic Resonance (NMR) spectroscopy, and Electron Ionization Mass Spectrometry (EI-MS). *n*-hexane, chloroform, ethyl acetate, acetone, and water extracts of the leaves of *G. hombroniana* were tested for their antioxidant activities using the total phenolic content (TPC), total flavonoid content (TFC) and 2,2-diphenyl-1-picrylhydrazyl (DPPH) radical scavenging activity assays, and also the anti-Alzheimer (cholinesterase) activities. All extracts showed weak antioxidant activities with inhibition less than 60%. Meanwhile, 50-75% of inhibition against AChE was observed, indicating a weak Alzheimer's disease inhibition.

**Key words:** *Garcinia hombroniana*; phytochemical; antioxidant; scavenging; anti-Alzheimer

Received: March 2020; Accepted: June 2020

Bioactive compounds extracted from plants have the property to scavenge free radicals. Compounds such as phenols are stable chemical species which are able to stop the oxidation reaction by donating hydrogen atoms to radical compounds. *Garcinia* species are among the most important plants with such source of bioactive chemical compounds [1].

Genus of *Garcinia* are widely distributed in tropical Asia, Africa, and Polynesia. More than 100 species of *Garcinia* have been reported and most of them are found in Southeast Asia, especially in Malaysia, Cambodia, Thailand, and Vietnam [2]. The *Garcinia* species were once classified as *Rheedea* in America. In Malaysia alone, there are 49 *Garcinia* species gathered out of 400 species estimated worldwide [3]. The applications of plants from this genus can be seen in culinary, pharmaceutical, and other industries. This genus comprises many groups of medicinal plants with therapeutic properties. Due to their remedial properties, the genus has received considerable attention from pharmaceutical industries. Different parts of the tree, such as bark, fruits, leaves, roots, and stems have been widely used to treat health problems. For example, the seeds of *G. kola* have been proven to cure hepatitis and used as cough medicine [4]. Another two species, *G. cowa* and *G. pedunculata* are often cultivated for their acidic fruits and the dried

slices of the fruits are used in culinary and the treatment of dysentery [5]. In Peninsular Malaysia, the fruits of *G. atroviridis*, also known as 'asam gelugor', are widely used in seasoning purposes. The leaves of *G. atroviridis* can either be cooked or consumed raw as salad [6-7]. *G. mangostana* or 'manggis' is known as the queen of fruits in Malaysia. The fruit hull of this plant has been used in Thai medicine, in the treatment of skin infections, wounds, and diarrhea [8]. Xanthenes, flavonoids, benzophenones, lactones, and phenolic acids are some of the secondary metabolites that have been isolated from the genus *Garcinia*. These phytochemical constituents in various *Garcinia* species have been reported to have bioactive compounds to treat health disorders such as inflammation, microbial infection, cancer, obesity, malaria, and others [9].

Elya *et al.* (2012) investigated the antioxidant activity of the extracts (*n*-hexane, ethyl acetate and methanol extracts) from the leaves of three different species; *G. hombroniana* Pierre, *G. lateriflora* Blume var. *Javanica* Boerl, and *G. kydia* Roxb [10]. All extracts from the three species of *Garcinia* showed positive results in the DPPH assay. The methanol extract showed the highest activity of all the three species. However, further screening was needed to identify the bioactive compound responsible for the

antioxidant activities. In 2011, Subhashini *et al.* studied the effects of using different concentrations of water extract of (fruit rinds) *G. combogia* on antioxidant activities. Although the study was carried out only on the water extract, there were still traces of antioxidant activities due to the presence of phenolic components in the extract [11]. The roots of *G. multiflora* were reported to show significant antioxidant activities. Wu *et al.* (2008) reported the antioxidant activities of different extracts from this plant, whereby the ethyl acetate extract possessed the highest antioxidant activities in comparison to the butanol and water extracts of the roots of *G. multiflora* [12]. Nevertheless, such results imply that the extracts from *G. multiflora* roots have great potentials to prevent diseases caused by overproduction of radicals. The published finding from Jamila *et al.* (2013) reported on the antioxidant activities of the bark extracts of *G. hombroniana* [13]. The DPPH assay was used in the determination of radical scavenging activities of the plant extracts. This assay was carried out on *n*-hexane, dichloromethane, ethyl acetate, methanol, and water extracts. The DPPH and TPC assays indicated that polar extracts from *G. hombroniana* possessed antioxidant properties. Meanwhile, Jamila *et al.* (2017) investigated the *in vivo* hepatoprotective and *in vitro* cytotoxic activities of methanolic ethyl acetate (MEA) *G. hombroniana* bark extract [14]. They found that MEA extract has a potential to inhibit the cytotoxicity behavior. The latest research was reported by Muhammad *et al.* (2019) on phytochemical studies of the stem bark of *G. parvifolia* and pericarp of *G. hombroniana* [15]. The results showed that the acetone extract was the most significant for antibacterial activities.

Alzheimer's disease is one of the neurodegenerative diseases that can be related to older citizens with dementia [16]. The neurotransmitter in the transmission signal at the synapse is called acetylcholine. Large amounts of acetylcholinesterase (AChE) and butyrylcholinesterase (BChE) enzymes terminate the pharmacological action of acetylcholine [17]. Investigations have been carried to discover more AChE and BChE inhibitors from natural plant resources, thus leads to alternatives in the treatment of Alzheimer's disease. Not many research works have been conducted on the anticholinesterase studies of *Garcinia*, in particular *G. hombroniana*. To date, only one study was reported. Jamila *et al.* (2013) reported the effects of using different extracts, namely *n*-hexane, dichloromethane, ethyl acetate, methanol, and water extracts from the bark of *G. hombroniana*. Results showed that all the bark extracts have some pharmacological activities which have the potential to become a new source of phytomedicine in fighting this disease [13].

In search for bioactive compounds, the choice and availability of a plant to be investigated is very important. The early stage investigation in phytochemistry might have bioactive characteristics

that can be related to their therapeutic applications. Older strategies for research in the area of natural products involve extraction and isolation of as many pure compounds as possible, identification of their chemical structures, and investigation of their biological properties. Even though a great number of systematic works have been carried out, a larger fraction still remains uninvestigated. The modern strategy, however, is a bioassay guided method, which means extracts with promising bioactive compounds are chosen, followed by isolation, identification, and biological assays of pure compounds. Research on the phytochemical and biological activity studies of the *Garcinia* genus has led to many findings. Many types of compounds were isolated and most of them showed good biological activities. However, not much work on *G. hombroniana* has been reported. The only hitherto reported work was the chemical structures of compounds isolated from the leaves of *G. hombroniana* [18]. However, no information about the biological activities of the compounds was provided. Hence, the present research work focuses on the isolation of some bioactive compounds from the leaves of *G. hombroniana*. Limited information regarding biological activities of the plant from this species justifies the need for further investigations on antioxidant and anticholinesterase activities of extracts from the leaves of *G. hombroniana*.

## MATERIALS AND METHODS

### 1. Instruments

FTIR spectroscopy was used to determine the functional groups of compounds and the IR spectra were recorded using Perkin-Elmer System 2000 FT-IR spectrometer. All spectra were obtained using the disc technique, by pressing potassium bromide and scanned in the range of 650 to 4000  $\text{cm}^{-1}$ . The molecular structures of all the compounds were determined using NMR spectroscopy [19]. The 1D NMR ( $^1\text{H-NMR}$ ,  $^{13}\text{C-NMR}$ , and DEPT) and 2D NMR (COSY, HMQC and HMBC) spectra were recorded using Bruker Advance 500 Spectrometer. MS analysis via electron ionization (EI) technique was carried out using Agilent Mass spectrometer 5975C MSD with a direct probe. In the total phenolic content (TPC) and radical scavenging capacity (DPPH) assays, absorbance was measured using UV-1800 Shimadzu Spectrophotometer. For TFC determination, absorbance was measured using UV/VIS Perkin Elmer Lambda 25 Spectrometer. In the cholinesterase inhibitory study, absorbance of samples was measured using Tecan Infinite 200 Pro Microplate Spectrophotometer. All the excess solvent in the extraction process was removed by Heidolph Instruments Laborota 4000-efficient rotary evaporator. The weight and melting points of all the samples were measured using GR-200 A&D Company and Stuart Scientific melting point apparatus, respectively. Spots on TLC plates were visualized with CC-10 UVP UV lamp. Further staining of the TLC plates needed heating using

BOSCH PHG 530-2 heat gun. The pH of all the samples was measured using Schott Instruments Lab 850 pH meter.

## 2. Plant Materials

Fresh leaves of *G. hombroniana* were collected from Penang Botanical Garden, Malaysia. The plant was identified at the Herbarium Department, Penang Botanical Garden with a voucher number PBGK12.

## 3. Extraction and Isolation of the Leaves of *G. hombroniana*

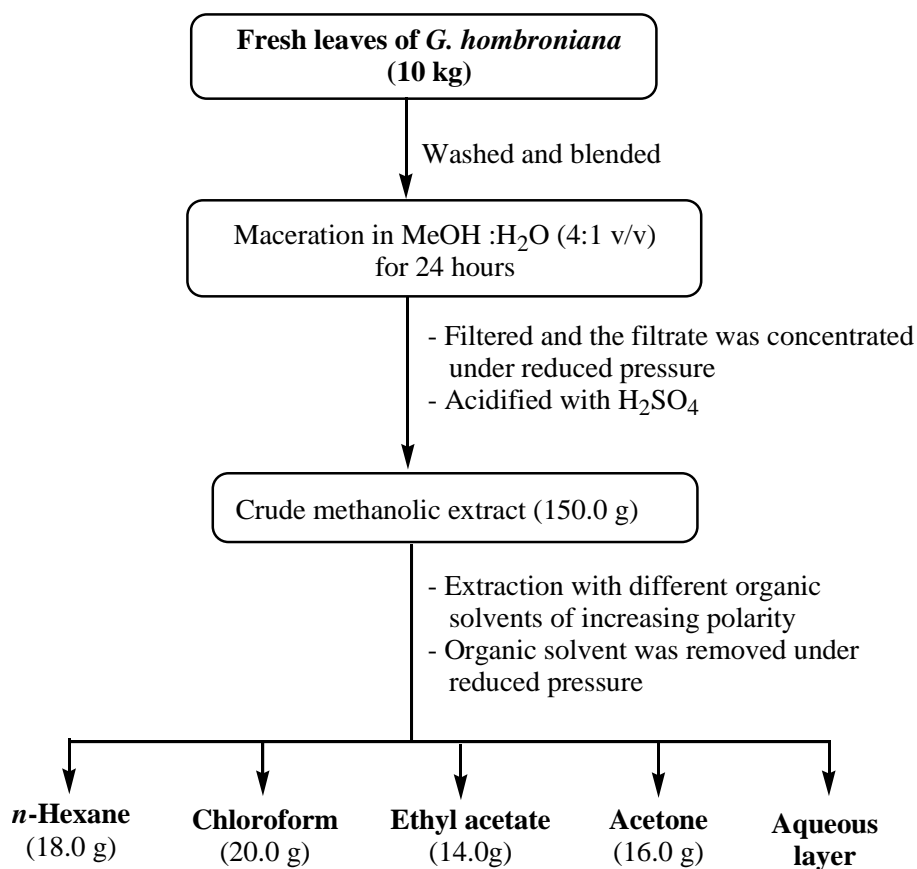
About 10 kg of leaves was cleaned to remove soil and other debris, which was then shredded in a blender into fine pieces. This was to increase the efficiency of extraction by increasing the surface area and facilitate the penetration of solvents into the cells. Subsequently, the leaves were macerated in a mixture of methanol:water (4:1 v/v) for 24 hours at room temperature. The methanol extract was then collected via filtration in a flask. This procedure was repeated three times [14].

The combined crude methanol extract was then concentrated to 1/10 of the initial volume using a rotary evaporator. The methanolic extract (150.0 g)

was then acidified to pH 6.5 with sulphuric acid, followed by extraction with *n*-hexane (3 × 200 mL). The organic layer was collected and evaporated till dryness to afford the *n*-hexane extract (18.0 g). The aqueous layer was further extracted with chloroform to give 20.0 g of extract, followed by ethyl acetate and acetone to produce 14.0 and 16.0 g of extracts, respectively. The extraction process is illustrated in Scheme 1.

## 4. Thin Layer Chromatography (TLC) Analysis of the Chloroform Extract

The chloroform extract (20.0 g) was subjected to thin layer chromatography (TLC), which was performed on pre-coated TLC plates (20 × 20 cm, coated with 0.2 mm silica gel F<sub>254</sub> on aluminium sheets, Merck) with silica gel as the stationary phase. The chloroform extract was subjected to column chromatography on a silica gel using gradient of increasing polarity with *n*-hexane-EtOAc-MeOH (1:0:0→0:0:1 v/v) as solvent. TLC plates were developed in a 20 mL beaker with 5.0 mL of solvent as the mobile phase [13]. Developed TLC plates were visualized by ultraviolet (UV) light at 254 nm. A mixture of methanol and concentrated sulphuric acid (5% H<sub>2</sub>SO<sub>4</sub>) was used as a staining reagent and TLC plates were heated with a heat gun.



**Scheme 1.** Flow chart of compound extraction of the leaves of *G. hombroniana*

### 5. Purification of the Chloroform Extract using Column Chromatography

Chromatographic separation was performed in a glass column (5.0 cm diameter  $\times$  120 cm height) loaded with silica gel, which was prepared by mixing silica gel with hexane and this silica gel slurry was packed into the glass column. The chloroform extract (20.0 g) was impregnated with silica gel (100-200 mesh, R&M Chemicals) and was loaded on the top of the packed silica gel in the column. The chloroform extract was chromatographed using *n*-hexane-EtOAc-MeOH solvent system to give fractions. Fractions eluted from the column were evaporated using a rotary evaporator. Some of the fractions containing pure compounds were re-crystallized but those with mixtures of compounds were re-chromatographed to separate the pure compounds. The flow chart of purification of the chloroform extract is shown in Scheme 2.

The first 300 fractions were grouped to form only 23 fractions based on their TLC profiles, labelled as fraction A (FA) to fraction W (FW). FA (232 mg, fractions 1 to 3) was evaporated to give a yellow solid when re-crystallized with methanol and chloroform (1:1 v/v) gave white needles of **CP-1** (97 mg,  $9.7 \times 10^{-4}$  %).

FC (279 mg, fractions 5 to 23) was evaporated to give a yellow solid and was re-crystallized from methanol and chloroform (1:1 v/v) to give **CP-2** (113 mg,  $1.1 \times 10^{-4}$  %), a white crystalline needle. FD (309 mg, fractions 24 to 46) was further re-chromatographed using solvents *n*-hexane and ethyl acetate to afford 27 sub-fractions of FD1 to FD27. Sub-fractions FD4 to FD6 were pooled together and evaporated to afford a solid crude, which was further re-crystallized from hexane and chloroform (1:1 v/v)

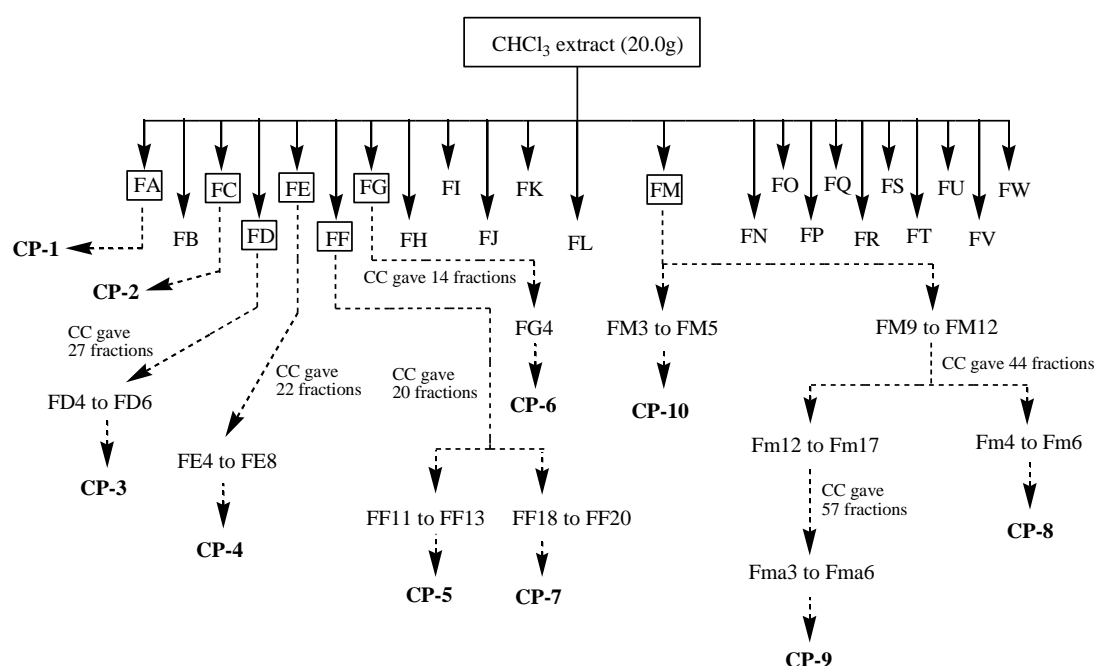
to give a white solid, **CP-3** (14 mg,  $1.4 \times 10^{-4}$  %).

**CP-4** (1.7 mg,  $1.7 \times 10^{-4}$  %) was obtained from the re-chromatographed of FE (241 mg, fractions 47 to 71). 22 sub-fractions were tested with TLC and fractions FE4 to FE8 were found to be almost pure. Recrystallization of the solid obtained using chloroform and methanol (1:1 v/v) afforded a white solid.

Greenish sticky extract of FF (617 mg, fractions 72 to 114) was re-chromatographed to afford 20 sub-fractions, FF1 to FF20. Sub-fractions FF11 to FF13 and FF18 to FF20 were combined separately. Both combinations of extracts were re-crystallized from methanol and mixture of methanol and chloroform (1:1 v/v) to afford **CP-5** (29 mg,  $2.9 \times 10^{-4}$  %) and **CP-7** (19 mg,  $1.9 \times 10^{-4}$  %), respectively.

FG (350 mg, fractions 115 to 143) was re-chromatographed to give 14 sub-fractions. One of the sub-fractions, FG4 was evaporated and the extract was re-crystallized from methanol, to give **CP-6** (23 mg,  $2.3 \times 10^{-4}$  %).

FM (753 mg, fractions 185 to 196) was re-chromatographed to give 17 sub-fractions. Sub-fractions FM3 to FM5 was grouped and recrystallized to give **CP-10** (43 mg,  $4.3 \times 10^{-4}$  %). Fractions FM12 to FM19 were grouped and re-chromatographed to give 44 sub-fractions, Fm1 to Fm44. **CP-8** (15 mg,  $1.5 \times 10^{-4}$  %) was obtained from sub-fractions Fm4 to Fm6 after the evaporation and re-crystallization from chloroform and methanol (1:1 v/v). Fractions Fm12 to Fm17 were re-chromatographed to afford **CP-9** (6 mg,  $6.0 \times 10^{-5}$  %), which was later re-crystallized from methanol.



Scheme 2. Flow chart of purification of the chloroform extract

*n*-hexane was the most nonpolar solvent used in the compound extraction of the leaves of *G. hombroniana*. Compounds extracted from this solvent were mostly lipophilic. A medium-polarity solvent, ethyl acetate, was used to extract compounds with intermediate polarity oxygenated compounds, namely diterpenoids and triterpenoids. More polar compounds were extracted using more polar solvents, namely acetone and water. Based on the TLC profiles of *n*-hexane, ethyl acetate, acetone, and water extracts, they showed poor separation using different mixtures of solvents as eluents. Based on the results from the quantification of TPC and TFC assays, the chloroform extract showed the most promising result in isolating compounds.

## 6. Total Phenolic Content (TPC) Assay

In the phenolic content determination, a calibration curve was constructed using the absorbance of gallic acid of known concentrations. A stock solution of 1000 µg/mL of gallic acid was prepared. Gallic acid (3 mg) was dissolved in 3 mL of MeOH. In between uses, this stock solution was protected from light by covering it with aluminium foil with a tightly sealed cap. It was prepared weekly and stored at 4°C in a refrigerator and the estimated time for it to maintain its potency was two weeks. Storage exceeding this period of time would result in a decrease in potency of the solution by 5%. A similar decrease in potency was observed in one week if the solution was kept at room temperature. Standard solutions of gallic acid of seven different concentrations, 10, 20, 40, 50, 60, 80, and 100 µg/mL, were prepared. A standard curve of various concentrations of gallic acid against the absorbance of gallic acid at 725 nm was plotted.

In order to construct a calibration curve, 150 µL of each standard solution was pipetted into individual test tubes. 2400 µL of ultra-pure water was then added to the test tubes and the contents were mixed well. 150 µL of 0.25 N Folin-Ciocalteu reagent was then added and mixed well. After three minutes, 300 µL of 1 N Na<sub>2</sub>CO<sub>3</sub> (aq) was added and mixed well and incubated in the dark for two hours. The absorbance of each solution was taken at 725 nm using UV-1800 Shimadzu spectrophotometer. Results were calculated using the following equation:

$$\text{TPC} = \frac{cV}{m}$$

In the above equation, TPC is the total amount of phenolic content; *c* is the concentration of gallic acid in mg/mL obtained from the calibration curve; *V* is the volume of extract in mL; and *m* is the weight of extract in g.

The total phenolic contents of *n*-hexane, CHCl<sub>3</sub>, EtOAc, acetone, and water extracts of *G. hombroniana* were determined using the Folin-Ciocalteu method. In individual test tubes, 150 µL of

each extract was diluted with 2400 µL of ultra-pure water and the contents were mixed well. 150 µL of 0.25 N Folin-Ciocalteu reagent was then introduced and the mixtures were mixed well. After three minutes, 300 µL of 1 N Na<sub>2</sub>CO<sub>3</sub> (aq) was added and the mixtures were shaken vigorously and incubated in the dark for two hours. The absorbance of each sample was determined at 725 nm using UV-1800 Shimadzu spectrophotometer. Gallic acid with concentrations ranging from 0.01 to 0.1 mg/mL was used as standards. The results were expressed as mg gallic acid equivalent (GAE /g of fresh mass). Additional dilutions were needed if the TPC values measured were beyond the concentration range of the standard curve.

## 7. Total Flavonoid Content (TFC) Assay

In the determination of total flavonoid content, quercetin was selected as the reference. Absorbance of six quercetin solutions of known concentrations was used to construct a calibration curve. A stock solution of quercetin at 4000 µg/mL was prepared by adding 10 mL of DMSO to 40 mg of quercetin in a volumetric flask until the latter was fully dissolved. This freshly prepared stock solution must be protected from light and kept in a refrigerator. Hence, it was stored in a vial with a tightly sealed cap. The stock solution was then diluted to give six solutions of different concentrations, 75, 100, 200, 500, 750, and 1000 µg/mL, with which the calibration curve was plotted. The calibration curve was plotted with different concentrations of quercetin at the absorbance of 510 nm.

To construct the calibration curve, 250 µL of each of the standard solutions of quercetin was pipetted into individual test tubes. 2250 µL of ultra-pure water was then added into the test tubes and the contents were mixed well. Then, the sample solutions were mixed with 150 µL of 5% NaNO<sub>2</sub> (w/w). After five minutes, 300 µL of 10% AlCl<sub>3</sub> (w/w) was added followed by 1000 µL of 1 M NaOH (aq). Finally, 1050 µL of ultra-pure water was added to make the total volume of the sample solutions to 5000 µL. Each test sample was prepared in triplicate. All the samples were then incubated in the dark for 30 minutes. The absorbance of each sample was then measured against a blank at 510 nm by a Perkin Elmer UV/VIS spectrophotometer. The calculation in this assay is similar to that in the TPC assay.

*n*-hexane, chloroform, ethyl acetate, acetone, and water extracts were assayed for their total flavonoid contents (TFC). In individual test tubes, the initial volume of each extract was increased from 250 µL to 2500 µL with ultra-pure water. Initially, to the test tubes, 150 µL of 5% NaNO<sub>2</sub> (w/w) was added. After five minutes, 300 µL of 10% AlCl<sub>3</sub> (w/w) was added, followed by the addition of 1000 µL of 1 M NaOH in ultra-pure water. The final adjustment was made to a total volume of 5000 µL. Absorbance was

measured at 510 nm using Perkin Elmer UV/VIS spectrometer Lambda 25. The standard used in this analysis was quercetin. The concentrations of quercetin solutions were from 0.075 mg/mL to 1.000 mg/mL. The results were expressed as mg quercetin equivalent (QE/g of fresh mass). Additional dilutions were needed if the TFC values measured were beyond the concentration range of the standard curve.

### 8. Determination of Radical Scavenging Activity (DPPH) Assay of the Chloroform Extract

The evaluation of the radical scavenging capacity (DPPH) assay on *n*-hexane, chloroform, ethyl acetate, acetone, and water extracts was done based on the method proposed by Brand-Williams *et al.* [20]. In this assay, Trolox was selected as the reference. A stock solution of Trolox with a concentration of 1000  $\mu$ M was prepared. 2.50 mg of Trolox was weighed and dissolved in 10 mL of methanol. This stock solution was kept in a refrigerator, and protected from light. The stock solution was then diluted to give five standard solutions: 25, 50, 100, 400, and 800  $\mu$ M. A standard curve of various concentrations of Trolox against the absorbance of Trolox at 515 nm was plotted.

A stock solution of DPPH was prepared by dissolving 24 mg of DPPH with 100 mL of methanol. The solution was then stored in a refrigerator until further use. In order to prepare the working solution, 10 mL of the DPPH stock solution was mixed with 45 mL of methanol. The absorbance of this solution was measured at the wavelength of 515 nm. The initial DPPH concentration in solution should give the absorbance of  $1.10 \pm 0.02$ .

In order to construct a calibration curve, 150  $\mu$ L of the different concentration standard solutions of Trolox was pipetted into five separate test tubes. 2850  $\mu$ L of the DPPH solution was then added to each of these test tubes and the contents were mixed well. All the samples were prepared in triplicates. The samples were then incubated in the dark for 24 hours. The absorbance of each sample was then measured against a blank using a UV-Shimadzu spectrophotometer at 515 nm. The capacity to scavenge DPPH radicals was calculated using the following equation:

$$\text{DPPH radical scavenging capacity (\%)} = \frac{\text{Abs}_{\text{control}} - \text{Abs}_{\text{sample}}}{\text{Abs}_{\text{control}}} \times 100$$

In the above equation,  $\text{Abs}_{\text{control}}$  is the absorbance of DPPH solution + methanol and  $\text{Abs}_{\text{sample}}$  is the absorbance of DPPH solution + extract or Trolox.

*n*-hexane, chloroform, ethyl acetate, acetone, and water extracts were used in the DPPH assay. 150  $\mu$ L of each extract was pipetted into individual test tubes. Subsequently, 2850  $\mu$ L of the DPPH solution was added to the test tubes and the contents were mixed well. All the samples were then incubated in

the dark for 24 hours. The absorbance of each sample was determined at 515 nm using UV-1800 Shimadzu spectrophotometer. A linear standard curve was obtained for Trolox solutions between 25 and 800  $\mu$ M. The results were expressed as  $\mu$ mol Trolox equivalent (TE/g of fresh mass). Additional dilutions were needed if the DPPH absorbance values measured were beyond the concentration range of the standard curve.

### 9. Acetylcholinesterase (AChE) Inhibition Assay of the Chloroform Extract

The acetylcholinesterase (AChE) inhibition of *n*-hexane, chloroform, ethyl acetate, acetone, and water extracts from the leaves of *G. hombroniana* was determined by the spectrophotometric method developed by Ellman *et al.* [21]. The microplate assay followed the method of Ahmed *et al.* with some modifications [22]. AChE from electric eel was used in this assay. Acetylthiocholine iodide (ATCI) was employed as a substrate to monitor the inhibition of AChE. 5,5'-Dithiobis [2-nitrobenzoic acid] (DTNB) was used in the measurement of AChE activity. Physostigmine, a standard AChE inhibitor, was used as a positive control. Solutions of test samples and control were prepared in DMSO. At 1% concentration, DMSO has no inhibitory effect on AChE. However, an increase in concentration beyond this value will affect the inhibition of AChE by preventing the hydrolysis of ATCI by this enzyme [23]. Each test was conducted in triplicates. Percentage inhibition of AChE was determined by comparing the reaction rate of the samples with that of the blank. The percentage inhibition was calculated using the following equation:

$$\text{Inhibition of AChE (\%)} = \frac{\text{Abs}_{\text{control}} - \text{Abs}_{\text{sample}}}{\text{Abs}_{\text{control}}} \times 100$$

In the equation,  $\text{Abs}_{\text{control}}$  is the absorbance of enzyme without a test sample and  $\text{Abs}_{\text{sample}}$  is the absorbance of enzyme with a test sample. AChE inhibitory activity of a sample was expressed in  $\text{IC}_{50}$  value ( $\mu$ g/mL or  $\mu$ M). This value represents the amount of a test sample required to inhibit the hydrolysis of the substrate, ATCI by 50%.

In the acetylcholinesterase inhibition assay, 140  $\mu$ L of 0.1 M sodium phosphate buffer (pH 8) was initially added to a 96-well microplate. Later, 20  $\mu$ L of each extract (test samples) was added to the microplate. This was followed by the addition of 20  $\mu$ L of 0.09  $\mu$ g/mL AChE solution. After incubation for 15 minutes at 25°C, 10  $\mu$ L of 10 mM of 5,5'-Dithiobis [2-nitrobenzoic acid] was added to each well. After five minutes, the reaction was then initiated with the addition of 10  $\mu$ L of 14 mM acetylthiocholine iodide. The hydrolysis of acetylthiocholine iodide was indicated by the formation of a yellow-colored end product. After the substrate has been added, the absorbance was measured using microplate spectrophotometer at 414 nm.

## 10. Statistical Analysis

All determinations for antioxidant and anticholinesterase studies including measurements of total phenolic content (TPC), total flavonoid content (TFC), radical scavenging capacity (DPPH), and cholinesterase inhibitory studies were conducted in triplicates. The reported values for each extract were calculated as mean  $\pm$  standard deviation (SD) of three independent experiments.

## RESULTS AND DISCUSSION

### 1. Structure Elucidation

The acidified methanolic extract was extracted with *n*-hexane (3  $\times$  200 mL). The organic layer was collected and evaporated till dryness to afford the *n*-hexane extract (18.0 g). The aqueous layer was further extracted with chloroform to give 20.0 g of extract, followed by ethyl acetate and acetone to produce 14.0 and 16.0 g of extracts, respectively

The chloroform extract was purified using thin layer chromatography and column chromatography, followed by the recrystallization technique afforded ten known compounds identified as friedelin (**CP-1**), stigmasterol (**CP-2**), taraxerol (**CP-3**), Garcihombronane D (**CP-4**), lupeol (**CP-5**), betulin (**CP-6**), betulinic acid (**CP-7**), stigmasterol glucoside (**CP-8**), 4-hydroxybenzoic acid (**CP-9**), and palmitic acid (**CP-10**). Structure elucidation of the molecular structure using 2D NMR (COSY, HMQC and HMBC) will be discussed only for selected compounds of **CP-8**.

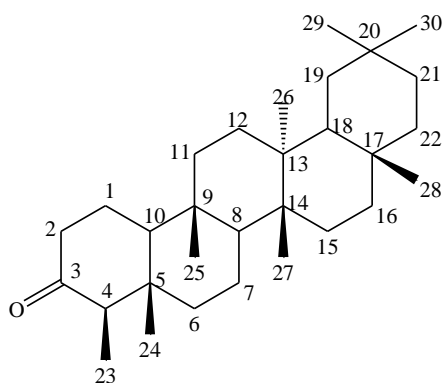


Figure 1. Structure of **CP-1** (Friedelin)

**CP-1**, as shown in Figure 1, was isolated from fraction FA (232 mg) by silica gel column chromatography, using hexane and ethyl acetate as eluents. A purple spot corresponding to **CP-1** was observed on the TLC plate with the  $R_f$  value of 0.45 (hexane:EtOAc; 4.75:0.25 v/v), thus suggesting a terpene [24]. Recrystallization of crude **CP-1** from MeOH and  $\text{CHCl}_3$  (1:1 v/v) gave white needles (97 mg,  $9.7 \times 10^{-4}$  %) with a melting point of 260-262°C [literature mp: 260-263°C [25]]. The mass spectrum (EI-MS) of **CP-1** showed a molecular ion peak at  $m/z$

426, which corresponded to a molecular formula of  $\text{C}_{30}\text{H}_{50}\text{O}$ . The degree of unsaturation for this compound was six, which suggested the presence of five cyclohexane fused rings and one carbonyl unit attached to one of the rings. The IR spectrum of this compound displayed the characteristic absorption bands at 2927, 2870, 1715, and 1390  $\text{cm}^{-1}$ . Absorption bands at 2870 and 2927  $\text{cm}^{-1}$  were attributed to the symmetrical and unsymmetrical stretching of  $\text{C}_{\text{sp}^3}\text{-H}$ , while a strong absorption at 1715  $\text{cm}^{-1}$  corresponded to the C=O stretching.

The  $^1\text{H-NMR}$  spectra of **CP-1** indicated the presence of eight methyl groups at  $\delta_{\text{H}}$  1.18, 1.05 (H-27), 1.00 (H-29 and H-26), 0.95 (H-30), 0.88 (H-25), 0.87 (H-23), and 0.73 (H-24) ppm. A pair of deshielded, non-equivalent methylene protons, H-2 was observed at 2.27 (H-2a) and 2.41 (H-2b) ppm (dd,  $J = 13.3, 5.0$  Hz), while a signal at 2.23 ppm was assigned to a methine proton, H-4. The  $^{13}\text{C-NMR}$  spectrum of **CP-1** showed 30 carbon signals. A signal at 213.31 ppm was assigned to a carbonyl carbon (C-3). The absence of  $sp^2$  carbon peaks confirmed the absence of a double bond. Spectral analyses of DEPT experiments indicated that 23 out of 30 carbon atoms in **CP-1** were attached to protons, comprising of eight methyl, 11 methylene, four methine, and seven quaternary carbons. Based on these observations, compound **CP-1** was concluded to be friedelin-3-one, also generally known as friedelin.

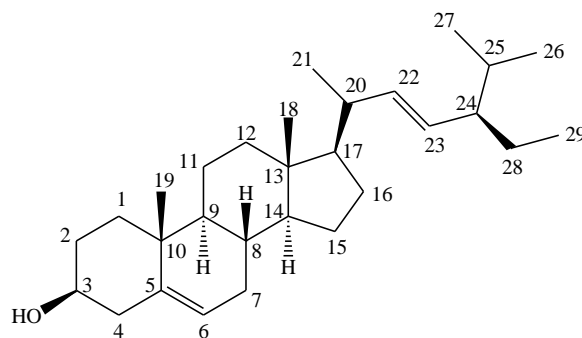


Figure 2. Structure of **CP-2** (Stigmasterol)

**CP-2** (Figure 2) was isolated from fraction FC (279 mg) by silica gel column chromatography, using hexane and ethyl acetate as eluents. A purple spot corresponding to **CP-2** was observed on the TLC plate with the  $R_f$  value of 0.67 (hexane:EtOAc; 9:1 v/v), thus suggesting a terpene [26]. Recrystallization of crude **CP-2** from MeOH and  $\text{CHCl}_3$  (1:1 v/v) gave white crystalline needles (113 mg,  $1.1 \times 10^{-3}$  %) with a melting point of 142-144°C [literature mp: 144-146°C [27]]. The mass spectrum (EI-MS) of **CP-2** showed a molecular ion peak at  $m/z$  412, which corresponded to a molecular formula of  $\text{C}_{29}\text{H}_{48}\text{O}$ . The degree of unsaturation of this compound was six, thus suggesting three cyclohexanes and a cyclopentane fused rings with one double bond in one of the rings

and another double bond in the side chain of the structure. The IR spectrum of this compound displayed several absorption bands at 3391, 1646, 1178, 1133, and 1042  $\text{cm}^{-1}$ . A broad absorption band at 3391  $\text{cm}^{-1}$  was attributed to the O-H stretching, while an absorption at 1646  $\text{cm}^{-1}$  was a result of the C=C stretching and a strong absorption at 1042  $\text{cm}^{-1}$  was due to the C-O stretching.

The  $^1\text{H-NMR}$  spectra of **CP-2** indicated the presence of six methyl groups at  $\delta_{\text{H}}$  1.03 (H-21), 1.01 (H-19), 0.85 (H-26), 0.81 (H-29 and H-27), and 0.70 (H-18). A signal for a methylene proton (H-6) was seen at  $\delta_{\text{H}}$  5.35. Two signals corresponding to olefinic protons (H-22 and H-23) of an exocyclic double bond were observed at  $\delta_{\text{H}}$  5.18 (dd,  $J = 15.2, 8.7$  Hz) and  $\delta_{\text{H}}$  5.04 (dd,  $J = 15.2, 8.7$  Hz), respectively. A multiplet at  $\delta_{\text{H}}$  3.49-3.55 was assigned to an oxymethine proton, H-3. The  $^{13}\text{C-NMR}$  spectrum showed 29 carbon signals. Signals attributable to  $sp^2$  carbons of the endocyclic double bond were seen in the downfield region of  $\delta_{\text{C}}$  140.78 (C-5) and 121.70 (C-6). Two signals at  $\delta_{\text{C}}$  138.29 and 129.33 were assigned to two olefinic carbons, C-22 and C-23, respectively. A characteristic signal at  $\delta_{\text{C}}$  71.82 corresponded to a carbinolic carbon, C-3. Spectral analyses of DEPT experiments indicated that 26 out of 29 carbon atoms in **CP-2** were attached to protons. The signals comprised of six methyl, nine methylene, 11 methine, and three quaternary carbons. Based on these interpretations, compound **CP-2** was concluded to be 5,22-stigmastadien-3 $\beta$ -ol, also generally known as stigmasterol.

All the  $^1\text{H}$  and  $^{13}\text{C-NMR}$  spectral data for **CP-2** were summarized and compared with those reported in the literature, as tabulated in Table 1.

**CP-3** was isolated from fractions FD4 to FD6 by silica gel column chromatography, using hexane and ethyl acetate as eluents. A purple spot of **CP-3** was observed on the TLC plate with the  $R_f$  value of 0.73 (hexane:EtOAc; 4:1 v/v), thus suggesting a terpene [29]. Recrystallization of crude **CP-3** from hexane and  $\text{CHCl}_3$  (1:1 v/v) gave a white solid ( $14 \text{ mg} \times 10^{-4} \%$ ) with a melting point of 242-244 $^\circ\text{C}$  [literature mp: 139-140 $^\circ\text{C}$  [30]]. The mass spectrum (EI-MS) of **CP-3** showed a molecular ion peak at  $m/z$  426, which corresponded to a molecular formula of  $\text{C}_{30}\text{H}_{50}\text{O}$ . The degree of unsaturation of this compound was six, thus suggesting five cyclohexane fused rings with one double bond in the ring. The IR spectrum of this compound displayed absorption bands at 3483, 2934, 2851, 1474, 1385, and 1038,  $\text{cm}^{-1}$ . A medium broad absorption band at 3483  $\text{cm}^{-1}$  was attributed to the O-H stretching of the hydroxyl group. Absorption bands at 2851 and 2934  $\text{cm}^{-1}$  were attributed to the symmetrical and unsymmetrical stretching of  $\text{C}_{\text{sp}^3}\text{-H}$ . Absorption at 1641  $\text{cm}^{-1}$  was a result of the C=C stretching, while absorptions at

1385 and 1474  $\text{cm}^{-1}$  were assigned to the bending of  $\text{C}_{\text{sp}^2}\text{-H}$  and  $\text{C}_{\text{sp}^3}\text{-H}$ , respectively.

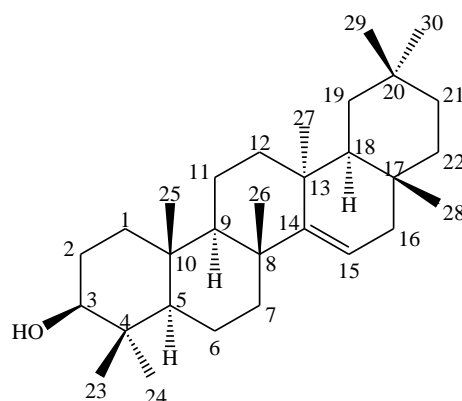


**Figure 3.** Structure of **CP-3** (Taraxerol)

Figure 3 shows the structure of **CP-3** with complete atomic numbering. The  $^1\text{H-NMR}$  spectra of **CP-3** indicated the presence of eight methyl groups at  $\delta_{\text{H}}$  1.09 (H-27), 0.98 (H-23), 0.95 (H-29), 0.93 (H-25), 0.91 (H-28 and H-30), 0.82 (H-26), and 0.80 (H-24) ppm. A signal ascribable to an olefinic proton of an endocyclic double bond (H-15) was observed at  $\delta_{\text{H}}$  5.54 as doublet of doublet (dd,  $J = 8.2, 3.2$  Hz). Another signal at  $\delta_{\text{H}}$  3.21 (dd,  $J = 11.3, 4.5$  Hz) was assigned to an oxymethine proton, H-3. One doublet of triplet which was observed at  $\delta_{\text{H}}$  2.05 (dt,  $J = 12.8, 3.2$  Hz) was assigned to a methylene proton (H-19b), while a doublet of doublet signal at  $\delta_{\text{H}}$  1.93 (dd,  $J = 14.7, 2.8$  Hz) was determined to be H-16b. The  $^{13}\text{C-NMR}$  spectrum showed 30 carbon signals.  $sp^2$  carbons of an endocyclic double bond was found to resonate in the downfield region at  $\delta_{\text{C}}$  158.11 (C-14) and 116.88 (C-15). A signal at  $\delta_{\text{C}}$  79.09 was assigned to a carbinolic carbon, C-3. Spectral analyses of DEPT experiments indicated that 23 out of 30 carbon atoms of **CP-3** were attached to protons. They comprised of eight methyl, ten methylene, five methine, and seven quaternary carbons. Based on these observations, compound **CP-3** was concluded to be 13 $\alpha$ -methyl-27-norolean-14-en-3 $\beta$ -ol, also generally known as taraxerol.

**CP-4** (Figure 4) was isolated from fractions FE4 to FE8 by silica gel column chromatography, using hexane and ethyl acetate as eluents. A purple spot of **CP-4** was observed on the TLC plate with the  $R_f$  value of 0.56 (hexane:EtOAc; 3:1 v/v), thus suggesting a terpene [31]. Recrystallization of crude **CP-4** from MeOH and  $\text{CHCl}_3$  (1:1 v/v) gave a white solid ( $17 \text{ mg}, 1.7 \times 10^{-4} \%$ ) with a melting point of 222-226 $^\circ\text{C}$  [literature mp: 218-220  $^\circ\text{C}$  [32]]. The mass spectrum (EI-MS) of **CP-4** showed a molecular ion peak at  $m/z$  426, which corresponded to a molecular formula of  $\text{C}_{30}\text{H}_{46}\text{O}_4$ . The degree of unsaturation for this compound was eight, thus suggesting three cyclohexanes and a cyclopentane fused rings, with



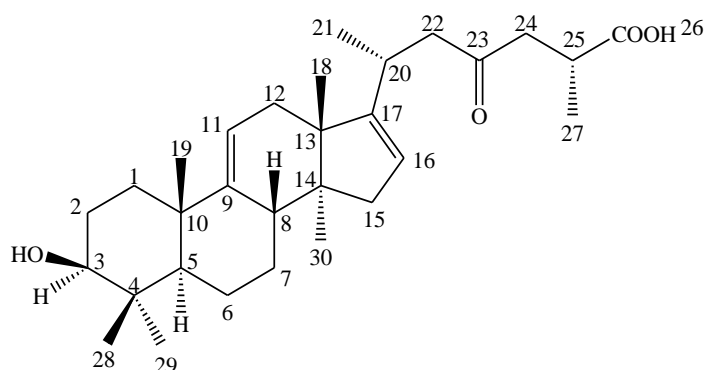


**Figure 4.** Structure of CP-4 (Garcihombronane D)

**Table 1.** A comparison of  $^1\text{H-NMR}$  and  $^{13}\text{C-NMR}$  spectral data (ppm) of CP-2 with those of stigmasterol<sup>a</sup>

Atom	$^1\text{H-NMR}$	$^1\text{H-NMR}^a$	$^{13}\text{C-NMR}$	$^{13}\text{C-NMR}^a$
1	1.84-1.86 (m, 1H), 1.06-1.08 (m, 1H)	1.84 (m, 1H), 1.08 (m, 1H)	37.28	37.6
2	1.83-1.86 (m, 1H), 1.51-1.52 (m, 1H)	1.83 (m, 1H), 1.51 (m, 1H)	31.70	31.9
3	3.49-3.55 (m, 1H)	3.51 (m, 1H)	71.82	72.0
4	2.29-2.31 (m, 1H), 2.21-2.23 (m, 1H)	2.30 (m, 1H), 2.23 (m, 1H)	42.34	42.5
5	-	-	140.78	140.8
6	5.34-5.36 (m, 1H)	5.34 (m, 1H)	121.70	121.8
7	1.97-1.98 (m, 1H), 1.51-1.52 (m, 1H)	1.97 (m, 1H), 1.50 (m, 1H)	31.91	21.1
8	1.47-1.50 (m, 1H)	1.46 (m, 1H)	31.93	32.2
9	0.93 (d, $J = 6.6$ Hz, 1H)	0.94 (m, 1H)	50.21	50.5
10	-	-	36.53	36.5
11	1.51-1.52 (m, 2H)	1.50 (m, 2H)	21.11	21.2
12	1.99-2.00 (m, 1H), 1.16-1.19 (m, 1H)	2.00 (m, 1H), 1.18 (m, 1H)	39.71	40.0
13	-	-	42.24	42.2
14	1.00-1.01 (m, 1H)	1.01 (m, 1H)	56.89	57.1
15	1.53-1.56 (m, 2H)	1.56 (m, 1H), 1.06 (m, 1H)	24.37	24.5
16	1.71-1.74 (m, 1H), 1.26-1.30 (m, 1H)	1.72 (m, 1H), 1.28 (m, 1H)	28.89	28.9
17	1.15-1.18 (m, 1H)	1.15 (q, 1H)	56.01	56.3
18	0.70 (s, 3H)	0.70 (s, 3H)	12.22	12.2
19	1.01 (s, 3H)	1.01 (s, 3H)	19.39	19.5
20	2.02-2.05 (m, 1H)	2.06 (m, 1H)	40.45	40.4
21	1.03 (s, 3H)	1.03 (d, 3H)	21.21	21.4
22	5.18 (dd, $J = 15.2, 8.7$ Hz, 1H)	5.17 (dd, $J = 15.2,$ 8.6 Hz, 1H)	138.29	138.3
23	5.04 (dd, $J = 15.1, 8.7$ Hz, 1H)	5.04 (dd, $J = 15.2,$ 8.6 Hz, 1H)	129.33	129.7
24	1.52-1.55 (m, 1H)	1.54 (m, 1H)	51.25	51.5
25	1.53-1.56 (m, 1H)	1.55 (m, 1H)	31.87	32.2
26	0.85-0.86 (m, 3H)	0.85 (d, 3H)	21.06	21.2
27	0.81 (s, 3H)	0.80 (d, 3H)	18.98	19.2
28	1.43-1.46 (m, 1H), 1.18-1.20 (m, 1H)	1.43 (m, 1H), 1.18 (m, 1H)	25.39	25.4
29	0.81 (s, 3H)	0.81 (t, 3H)	12.05	12.2

Note: <sup>a</sup>  $^1\text{H-NMR}$  and  $^{13}\text{C-NMR}$  spectral data reported in literature [28].

two double bonds in the ring and two carbonyl units in the side chain (ketone and carboxylic acid units). The IR spectrum of this compound displayed a broad overlapping absorption band at 3570 and 3364  $\text{cm}^{-1}$ , which referred to the O-H stretching for the hydroxyl and carboxylic acid groups. A weak absorption at 3053  $\text{cm}^{-1}$  was attributed to the  $\text{C}_{\text{sp}^2}\text{-H}$  stretching. Absorption bands at 2940 and 2969  $\text{cm}^{-1}$  were attributed to the symmetrical and unsymmetrical stretching of  $\text{C}_{\text{sp}^3}\text{-H}$ . A strong absorption at 1710  $\text{cm}^{-1}$  indicated the presence of the C=O stretching of ketone group while a moderate absorption band at 1628  $\text{cm}^{-1}$  indicated the presence of the C=C stretching.

The  $^1\text{H-NMR}$  spectra of **CP-4** indicated the presence of seven methyl groups at  $\delta_{\text{H}}$  1.05 (H-27), 1.01 (H-19), 0.96 (H-21), 0.90 (H-28), 0.75 (H-30), 0.73 (H-29), and 0.72 (H-18) ppm. Two signals for olefinic protons which represented an endocyclic double bond (H-11 and H-16) were displayed as broad doublet and broad singlet at  $\delta_{\text{H}}$  5.28 (d,  $J = 5.9$  Hz) and 5.25, respectively. Another signal at  $\delta_{\text{H}}$  3.02 (dd,  $J = 10.8, 4.9$  Hz) was assigned to an oxymethine proton, H-3. One doublet observed at  $\delta_{\text{H}}$  2.07 (d,  $J = 14.9$  Hz) was assigned to a methylene proton (H-15b), while a doublet of doublet signal at  $\delta_{\text{H}}$  1.81 (dd,  $J = 14.9, 3.0$  Hz) was determined to be H-15a. The  $^{13}\text{C-NMR}$  spectrum of **CP-4** showed 30 carbon signals. One carbonyl carbon for ketone peak was found to resonate in the downfield region, at  $\delta_{\text{C}}$  207.88 (C-23). Another carbonyl carbon for the acid group in this compound appeared at  $\delta_{\text{C}}$  176.65 (C-26).  $\text{sp}^2$  carbons which represented an endocyclic double bond were observed at  $\delta_{\text{C}}$  155.39 (C-17), 149.47 (C-9), 119.84 (C-16), and 113.69 (C-11). Another signal at  $\delta_{\text{C}}$  78.84 was designated to an oxygenated carbon (C-3). Spectral analyses of DEPT experiments indicated that 22 out of 30 carbon atoms in **CP-4** were attached to protons. They comprised of seven methyl, eight methylene, seven methine, and eight quaternary carbons.

Based on these observations and spectral interpretations, compound **CP-4** was concluded to be 3 $\beta$ -hydroxy-23-oxo-9,16-lanostandien-26-oic acid, also known as garciahombronane D, as shown in Figure 4.

**CP-5** was isolated from fractions FF11 to FF13 by silica gel column chromatography, using hexane and ethyl acetate as eluents. A purple spot corresponding to **CP-5** was observed on the TLC plate with the  $R_{\text{f}}$  value of 0.54 (hexane:EtOAc; 4:1 v/v), thus suggesting a terpene [33]. Recrystallization of crude **CP-5** from MeOH gave a white powder (29 mg,  $2.9 \times 10^{-4}$  %) with a m.p. of 213-215 $^{\circ}\text{C}$  {literature mp: 214-217 $^{\circ}\text{C}$  [34]}. The mass spectrum (EI-MS) showed a molecular ion peak at  $m/z$  426, which corresponded to the molecular formula of  $\text{C}_{30}\text{H}_{50}\text{O}$ . The degree of unsaturation of this compound was six, thus suggesting four cyclohexanes and a cyclopentane fused rings with one double bond in the side chain in its structure. The IR spectrum of this compound displayed a broad absorption band at 3366  $\text{cm}^{-1}$ , which

was attributed to the O-H stretching of the hydroxyl group. A weak absorption at 3050  $\text{cm}^{-1}$  was attributed to the  $\text{C}_{\text{sp}^2}\text{-H}$  stretching. Absorption bands at 2850 and 2944  $\text{cm}^{-1}$  were attributed to the symmetrical and unsymmetrical stretching of  $\text{C}_{\text{sp}^3}\text{-H}$ . A moderate absorption band at 1638  $\text{cm}^{-1}$  corresponded to the C=C stretching.

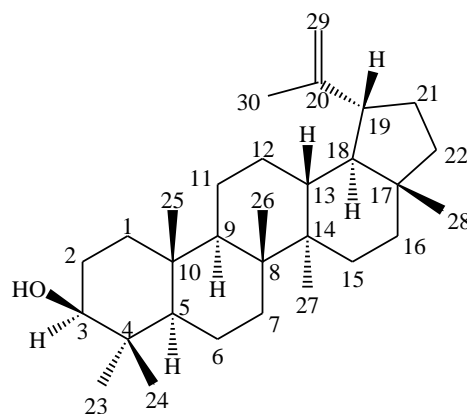


**Figure 5.** Structure of **CP-5** (Lupeol)

The complete atomic numbering of **CP-5** is shown in Figure 5. The  $^1\text{H-NMR}$  spectra of **CP-5** indicated the presence of seven methyl groups at  $\delta_{\text{H}}$  1.68 (H-30), 1.02 (H-26), 0.96 (H-23), 0.94 (H-27), 0.82 (H-25), 0.78 (H-28), and 0.75 (H-24). Two signals of olefinic protons corresponding to an exocyclic double bond (H-29) were observed as a doublet at  $\delta_{\text{H}}$  4.69 (d,  $J = 2.2$  Hz) and a singlet at  $\delta_{\text{H}}$  4.57. A signal at  $\delta_{\text{H}}$  3.20 (dd,  $J = 11.4, 4.9$  Hz) was assigned to an oxymethine proton, H-3. The  $^{13}\text{C-NMR}$  spectrum of **CP-5** showed 30 carbon signals. Two signals at  $\delta_{\text{C}}$  151.10 and 109.55 could be assigned to two olefinic carbons, C-20 and C-29, respectively. A deshielded signal at  $\delta_{\text{C}}$  151.10 was assigned to C-20 of a quaternary olefinic carbon. A signal at  $\delta_{\text{C}}$  79.20 was corresponded to a carbinolic carbon, C-3. Spectral analyses of DEPT experiments indicated that 24 out of 30 carbon atoms in **CP-5** were attached to protons. They comprised of seven methyl, 11 methylene, six methine, and six quaternary carbons. These confirmed that compound **CP-5** was 20(29)-lupeol-3 $\beta$ -ol, which is also identified as lupeol.

**CP-6** (Figure 6) was isolated from fraction FG4 by silica gel column chromatography, using hexane and ethyl acetate as eluents. A purple spot corresponding to **CP-6** was observed on the TLC plate with the  $R_{\text{f}}$  value of 0.63 (hexane:EtOAc; 7:3 v/v), thus suggesting a terpene [35]. Recrystallization of crude **CP-6** from methanol gave a white solid (23 mg,  $2.3 \times 10^{-4}$  %) with a melting point of 242-244 $^{\circ}\text{C}$  {literature mp: 242-246  $^{\circ}\text{C}$  [36]}. The mass spectrum (EI-MS) showed a molecular ion peak at  $m/z$  442, which corresponded to a molecular formula of  $\text{C}_{30}\text{H}_{50}\text{O}_2$ . The degree of unsaturation for this compound was six, thus suggesting four cyclohexanes and a cyclopentane fused rings with one double bond

in the side chain of its structure. The IR spectrum of this compound displayed a broad absorption band at  $3391\text{ cm}^{-1}$ , attributed to the O-H stretching. A very weak absorption at  $3050\text{ cm}^{-1}$  was attributed to the  $\text{C}_{\text{sp}^2}\text{-H}$  stretching. Absorption bands at  $2870$  and  $2943\text{ cm}^{-1}$  were attributed to the symmetrical and unsymmetrical stretching of  $\text{C}_{\text{sp}^3}\text{-H}$ . A moderate absorption band at  $1687\text{ cm}^{-1}$  indicated the presence of the C=C stretching.

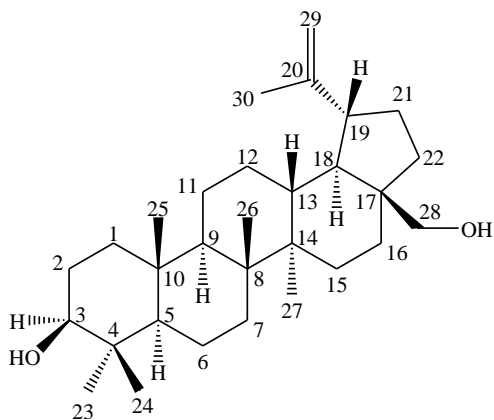


**Figure 6.** Structure of **CP-6** (Betulin)

The  $^1\text{H-NMR}$  spectra of **CP-6** indicated the presence of six methyl protons at  $\delta_{\text{H}}$  1.68 (H-30), 1.02 (H-26), 0.98 (H-27), 0.97 (H-23), 0.82 (H-25), and 0.76 (H-24) ppm. Signals ascribable to olefinic protons of an exocyclic double bond (H-29) were observed at  $\delta_{\text{H}}$  4.68 (d,  $J = 2.1$  Hz) and resonated as a singlet at  $\delta_{\text{H}}$  4.58. A signal at  $\delta_{\text{H}}$  3.20 (dd,  $J = 11.4, 4.9$  Hz) was assigned to an oxymethine proton, H-3. These characteristic signals suggested the structure of a lupane skeleton. Alongside the discussed signals, the spectra also showed two doublets which represented oxymethylene protons at  $\delta_{\text{H}}$  3.81 (d,  $J = 10.9$  Hz) and 3.34 (d,  $J = 10.8$  Hz) for H-28b and H-28a, respectively. The  $^{13}\text{C-NMR}$  spectrum of **CP-6** showed 30 carbon signals. Signals at  $\delta_{\text{C}}$  150.48 and 109.69 could be assigned to two olefinic carbons, C-20 and C-29, respectively. A deshielded signal at  $\delta_{\text{C}}$  150.48 was assigned to C-20 of a quaternary olefinic carbon characteristic, while a signal at  $\delta_{\text{C}}$  79.00 corresponded to a carbinolic carbon, C-3. A signal at  $\delta_{\text{C}}$  60.55 was assigned to a methylene carbon, C-28, containing a hydroxyl group. Spectral analyses of DEPT experiments indicated that 24 out of 30 carbon atoms in **CP-6** were attached to protons. They comprised of six methyl, 12 methylene, six methine, and six quaternary carbons.

Based on these observations, compound **CP-6** was concluded to be 20(29)-lup-en-3,28-diol, also generally known as betulin.

**CP-7** was isolated from fractions FF18 to FF20 by silica gel column chromatography, using hexane and ethyl acetate as eluents. A purple spot

corresponding to **CP-7** was observed on the TLC plate with the  $R_{\text{f}}$  value of 0.62 ( $\text{CHCl}_3\text{:MeOH}$ ; 9:1 v/v), thus suggesting a terpene [35]. Recrystallization of crude **CP-7** from MeOH and  $\text{CHCl}_3$  (1:1) gave a white solid (19 mg,  $1.9 \times 10^{-4}$  %) with a melting point of  $316\text{--}318^\circ\text{C}$  [literature mp:  $315\text{--}317^\circ\text{C}$  [37]]. The mass spectrum (EI-MS) showed a molecular ion peak at  $m/z$  456, which corresponded to a molecular formula of  $\text{C}_{37}\text{H}_{48}\text{O}_3$ . The degree of unsaturation for this compound was seven, thus suggesting four cyclohexanes and a cyclopentane fused rings with one double bond in the side chain and a carbonyl unit of the acid. The IR spectrum of this compound displayed a broad absorption band at  $3391\text{ cm}^{-1}$  attributed to the O-H stretching. A very weak absorption at  $3050\text{ cm}^{-1}$  was attributed to the  $\text{C}_{\text{sp}^2}\text{-H}$  stretching. Absorption bands at  $2870$  and  $2943\text{ cm}^{-1}$  were assigned to the symmetrical and unsymmetrical stretching of  $\text{C}_{\text{sp}^3}\text{-H}$ , while a moderate absorption band at  $1686\text{ cm}^{-1}$  indicated the presence of the C=C stretching.

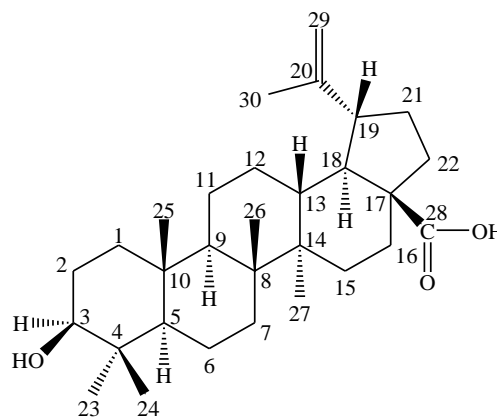


**Figure 7.** Structure of **CP-7** (Betulinic acid)

The structure of compound **CP-7** with complete numbering is shown in Figure 7. The  $^1\text{H-NMR}$  spectrum of **CP-7** indicated the presence of six methyl groups at  $\delta_{\text{H}}$  1.69 (H-30), 0.98 (H-27), 0.96 (H-23), 0.94 (H-26), 0.82 (H-25), and 0.75 (H-24) ppm. Two signals of olefinic protons corresponding to an exocyclic double bond (H-29) resonated as singlets at  $\delta_{\text{H}}$  4.74 and 4.61. A signal of double of doublet at  $\delta_{\text{H}}$  3.21 (dd,  $J = 11.4, 4.8$  Hz) was assigned to an oxymethine proton, H-3, while a multiplet observed at  $\delta_{\text{H}}$  3.00 was assigned to a methine proton, H-19. These chemical shifts were the characteristic peaks of lupane skeleton. The  $^{13}\text{C-NMR}$  spectrum of **CP-7** showed 30 carbon signals. The presence of a carbonyl carbon was observed in a deshielded region at  $\delta_{\text{C}}$  179.90. However, the absence of a methyl singlet, with the appearance of a carbonyl unit, suggested the presence of an acid group in its structure which could be assigned to the position of C-28. The characteristic pair of  $sp^2$  carbons which corresponded to an exocyclic double bond was observed at  $\delta_{\text{C}}$  150.67 (C-20) and 109.94 (C-29). A signal at  $\delta_{\text{C}}$  79.27 was assigned to an oxygenated carbon, C-3. Spectral

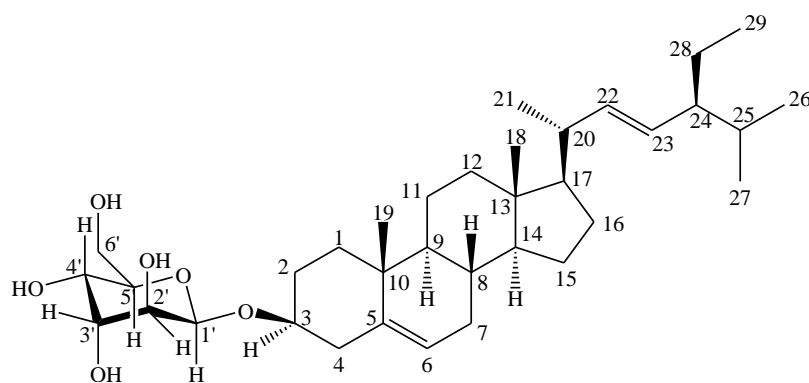


**Figure 8.** Structure of **CP-8** (Stigmasterol glucoside)

analyses of DEPT experiments indicated that 24 out of 30 carbon atoms in **CP-7** were attached to protons. They comprised of six methyl, twelve methylene, six methine, and six quaternary carbons.

The experimental data of NMR confirmed compound **CP-7** was 3 $\beta$ ,-dihydroxylup-20(29)-ene-28-oic acid, generally known as betulinic acid.

**CP-8** (Figure 8) was isolated from fractions Fm4 to Fm6 by silica gel column chromatography, using hexane and ethyl acetate as eluents. A purple spot corresponding to **CP-8** was observed on the TLC plate with the  $R_f$  value of 0.53 (EtOAc:MeOH; 4:1 v/v), thus suggesting a terpene [38]. Recrystallization of crude **CP-8** from MeOH and  $\text{CHCl}_3$  (1:1 v/v) gave a white crystal (15 mg,  $1.5 \times 10^{-4}$  %) with a melting point of 285-288°C [literature mp: 289-290°C [39]]. The mass spectrum (EI-MS) showed a molecular ion peak at  $m/z$  597  $[\text{M} + \text{Na}]^+$ , which corresponded to a molecular formula of  $\text{C}_{35}\text{H}_{58}\text{O}_6$ . The IR spectrum of this compound displayed a broad absorption band at  $3404\text{ cm}^{-1}$ , attributed to the O-H stretching of the hydroxyl group. Absorption bands at 2869 and  $2934\text{ cm}^{-1}$  were attributed to the symmetrical and unsymmetrical stretching of  $\text{C}_{\text{sp}^3}\text{-H}$ , while a moderate absorption at  $1460\text{ cm}^{-1}$  was assigned to the  $\text{C}=\text{C}$  stretching of the double bond.

The  $^1\text{H-NMR}$  spectra of **CP-8** indicated the presence of six methyl groups at  $\delta_{\text{H}}$  1.00 (H-21), 0.95 (H-19), 0.82 (H-29), 0.81 (H-27), 0.79 (H-26), and 0.67 (H-18) ppm. A signal corresponding to an olefinic proton of an endocyclic double bond, H-6 was found to resonate at  $\delta_{\text{H}}$  5.33 as a singlet. Another pair of olefinic protons, H-22 (dd,  $J = 15.1, 8.8\text{ Hz}$ ) and H-23 (dd,  $J = 15.1, 8.8\text{ Hz}$ ) of a side chain double bond, were observed as two doublet of doublets at  $\delta_{\text{H}}$  5.17 ( $J = 15.1, 8.7\text{ Hz}$ ) and 5.04 ( $J = 15.1, 8.8\text{ Hz}$ ), respectively. Another doublet ( $J = 7.8\text{ Hz}$ ) which was attributable to an anomeric hydrogen of the glucose moiety, H-1' appeared at  $\delta_{\text{H}}$  3.66. The  $^{13}\text{C-NMR}$  spectrum of **CP-8** showed 35 carbon signals, of which 29 carbons were assigned to the stigmasterol moiety, while the remaining six carbons were those of the sugar moiety. The most downfield signal at  $\delta_{\text{C}}$  140.53

ppm, a characteristic of a quaternary olefinic carbon, corresponded to C-5. Two signals at  $\delta_{\text{C}}$  138.11 and 128.91 were assigned to two olefinic carbons, C-22 and C-23, respectively. Another endocyclic olefinic carbon, C-6 appeared at  $\delta_{\text{C}}$  121.29. A signal at  $\delta_{\text{C}}$  100.85 was attributed to an anomeric carbon, C-1', which indicated the presence of a single monosaccharide moiety. Spectral analyses of DEPT experiments indicated that 32 out of 35 carbon atoms in **CP-8** were attached to protons. They comprised of six methyl, ten methylene, 16 methine, and three quaternary carbons.

COSY experiment (Figure 9) clearly exhibited the  $^1\text{H-}^1\text{H}$  correlations for proton signals at  $\delta_{\text{H}}$  5.33 (H-6) to  $\delta_{\text{H}}$  1.94 (H-7). A signal at  $\delta_{\text{H}}$  5.17 (H-22) yielded a cross peak to  $\delta_{\text{H}}$  5.04 (H-23). Two more cross peaks with strong intensities could be observed at  $\delta_{\text{H}}$  3.66 (H-6'b) with correlations to  $\delta_{\text{H}}$  3.40 (H-6'a) and 3.06 (H-5').

The assignments of the connectivity of carbons to their corresponding protons were confirmed using a HMQC spectrum (Figure 10). An olefinic proton at  $\delta_{\text{H}}$  5.33 (H-6) showed a strong correlation to a carbon resonating at  $\delta_{\text{C}}$  140.53 (C-6). Another pair of olefinic protons on a side chain at  $\delta_{\text{H}}$  5.17 and 5.04 were correlated to carbons at  $\delta_{\text{C}}$  138.11 and 128.91, thus assigning the positions as C-22 and C-23, respectively. A strong correlation was observed between a doublet originating from the glucose moiety,  $\delta_{\text{H}}$  3.66 (H-1') to  $\delta_{\text{C}}$  100.85 (C-1').

Relationships in the bonding structure were proven with long range correlation between protons and carbons in HMBC experiments (Figure 11). Three correlations were observed for a proton at  $\delta_{\text{H}}$  5.33 (H-6) with  $\delta_{\text{C}}$  38.38 (C-1) and 36.29 (C-10), while the other spot was shared between  $\delta_{\text{C}}$  31.49 (C-8) and 31.45 (C-7). In the spectrum, correlations of the olefinic protons at  $\delta_{\text{H}}$  5.17 (H-22) and 5.04 (H-23) appeared at  $\delta_{\text{C}}$  138.11 (C-23) and 128.91 (C-22), respectively. An anomeric proton at  $\delta_{\text{H}}$  4.23 (H-1') showed correlations to  $\delta_{\text{C}}$  76.82 (C-3') and 76.78 (C-5'), both from the structure of glucose.

The experimental data of NMR were compared to that reported in the literature, and based on all the analyses, compound **CP-8** was concluded to be stigmast-5,22-dien-3-O- $\beta$ -D-glucopyranoside, also

known as stigmasterol glucoside. All the  $^1\text{H}$  and  $^{13}\text{C}$ -NMR spectral data for **CP-8** were summarized and compared with those reported in the literature, as shown in Table 2.

**Table 2.** A comparison of  $^1\text{H}$ -NMR and  $^{13}\text{C}$ -NMR spectral data (ppm) of **CP-8** with those of stigmasterol glucoside<sup>b</sup>.

Atom	$^1\text{H}$ -NMR	$^1\text{H}$ -NMR <sup>b</sup>	$^{13}\text{C}$ -NMR	$^{13}\text{C}$ -NMR <sup>b</sup>
1	2.35-2.37 (m, 1H), 2.10-2.15 (m, 1H)	2.36 (m, 1H), 2.13 (m, 1H)	38.38	38..28
2	1.26-1.28 (m, 1H), 1.02-1.04 (m, 1H)	1.30 (m, 2H)	33.41	33.33
3	3.50 (overlapped, 1H)	3.42 (m, 1H)	77.05	76.95
4	1.78-1.83 (m, 1H), 1.02-1.04 (m, 1H)	1.80 (br. d, $J=10.2$ , 1H), 1.16 (br. d, $J=6.6$ Hz, 1H)	36.90	36.76
5	-	-	140.53	140.43
6	5.33 (s, 1H)	5.32 (br. d, $J=4.5$ Hz, 1H)	121.29	121.04
7	1.89-1.97 (m, 2H)	1.46 (m, 2H)	31.45	31.30
8	1.49-1.50 (m, 1H)	1.51 (br. s, 1H)	31.49	31.38
9	0.90 (d, $J=6.4$ Hz, 1H)	0.99 (br. s, 1H)	49.68	49.57
10	-	-	36.29	36.15
11	1.20-1.24 (m, 2H)	1.17 (m, 2H)	22.68	22.59
12	1.89-1.97 (m, 1H), 1.14-1.17 (m, 1H)	1.94 (m, 1H), 1.13 (m, 1H)	39.16	41.69
13	-	-	41.93	41.80
14	1.02-1.04 (m, 1H)	1.08 (m, 1H)	56.35	56.20
15	1.14-1.17 (m, 2H)	1.12 (m, 2H)	24.95	24.72
16	1.78-1.83 (m, 1H), 1.49-1.50 (m, 1H)	1.91 (br. s, 1H), 1.77(br. s, 1H)	29.33	29.20
17	1.02-1.04 (m, 1H)	1.01 (m, 1H)	55.50	56.11
18	0.67 (d, $J=10.0$ Hz, 3H)	0.65 (s, 3H)	12.20	11.76
19	0.95 (s, 3H)	0.99 (s, 3H)	19.01	18.99
20	1.26-1.28 (m, 1H)	1.34 (m, 1H)	35.55	35.37
21	1.00 (d, $J=6.6$ Hz, 3H)	0.91 (d, $J=6.3$ Hz, 3H)	18.69	18.76
22	5.17 (dd, $J=15.1, 8.8$ Hz, 1H)	5.18 (dd, $J=15.0, 8.4$ Hz, 1H)	138.11	137.85
23	5.04 (dd, $J=15.1, 8.8$ Hz, 1H)	5.04 (dd, $J=8.4, 8.1$ Hz, 1H)	128.91	128.79
24	0.90 (d, $J=6.4$ Hz, 1H)	0.99 (br. s, 1H)	45.22	31.20
25	1.38-1.41 (m, 1H)	1.63 (m, 1H)	31.41	31.20
26	0.79 (d, $J=6.3$ Hz, 3H)	0.84 (d, $J=6.3$ Hz, 3H)	19.17	19.28
27	0.81 (d, $J=3.2$ Hz, 3H)	0.80 (d, $J=6.9$ Hz, 3H)	18.92	18.89
28	1.49-1.50 (m, 1H), 1.02-1.04 (m, 1H)	1.01 (br. s, 2H)	23.94	23.76
29	0.82 (s, 3H)	0.79 (d, $J=8.1$ Hz, 3H)	11.74	11.58
1'	4.23 (d, $J=7.8$ Hz, 1H)	4.23 (d, $J=7.8$ Hz, 1H)	100.85	100.77
2'	3.00-3.04 (m, 1H)	2.91 (m, 1H)	70.17	70.14
3'	3.11-3.15 (m, 1H)	3.15 (m, 1H)	76.82	76.75
4'	2.88-2.91 (m, 1H)	3.08 (m, 1H)	73.53	73.43
5'	3.04-3.07 (m, 1H)	3.04 (m, 1H)	76.78	76.63
6'	3.66 (d, $J=11.3$ Hz, 1H), 3.40 (overlapped, 1H)	3.66 (m, 1H), 3.50 (m, 1H)	61.16	61.10

Note: <sup>b</sup>  $^1\text{H}$ -NMR and  $^{13}\text{C}$ -NMR spectral data reported in literature [40].

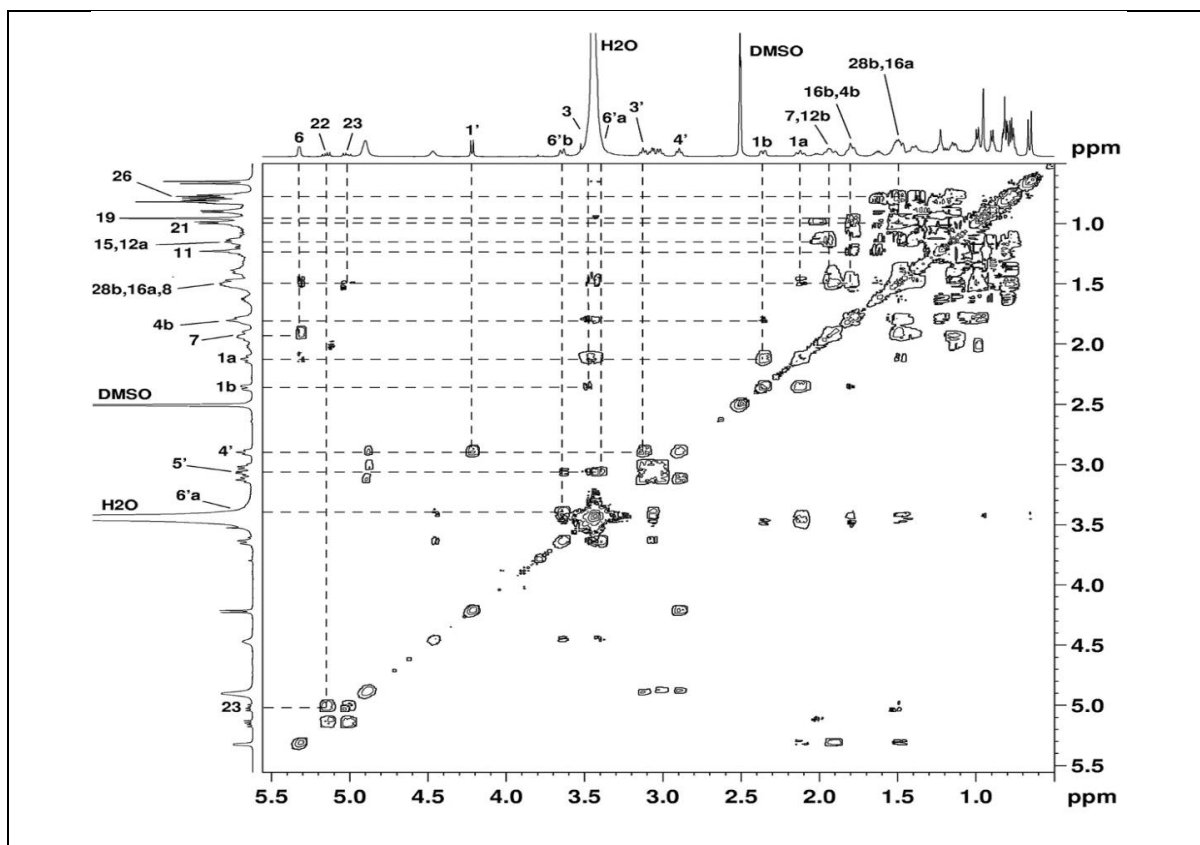


Figure 9. COSY ( $^1\text{H}$ - $^1\text{H}$ ) spectrum of CP-8 (DMSO- $d_6$ )

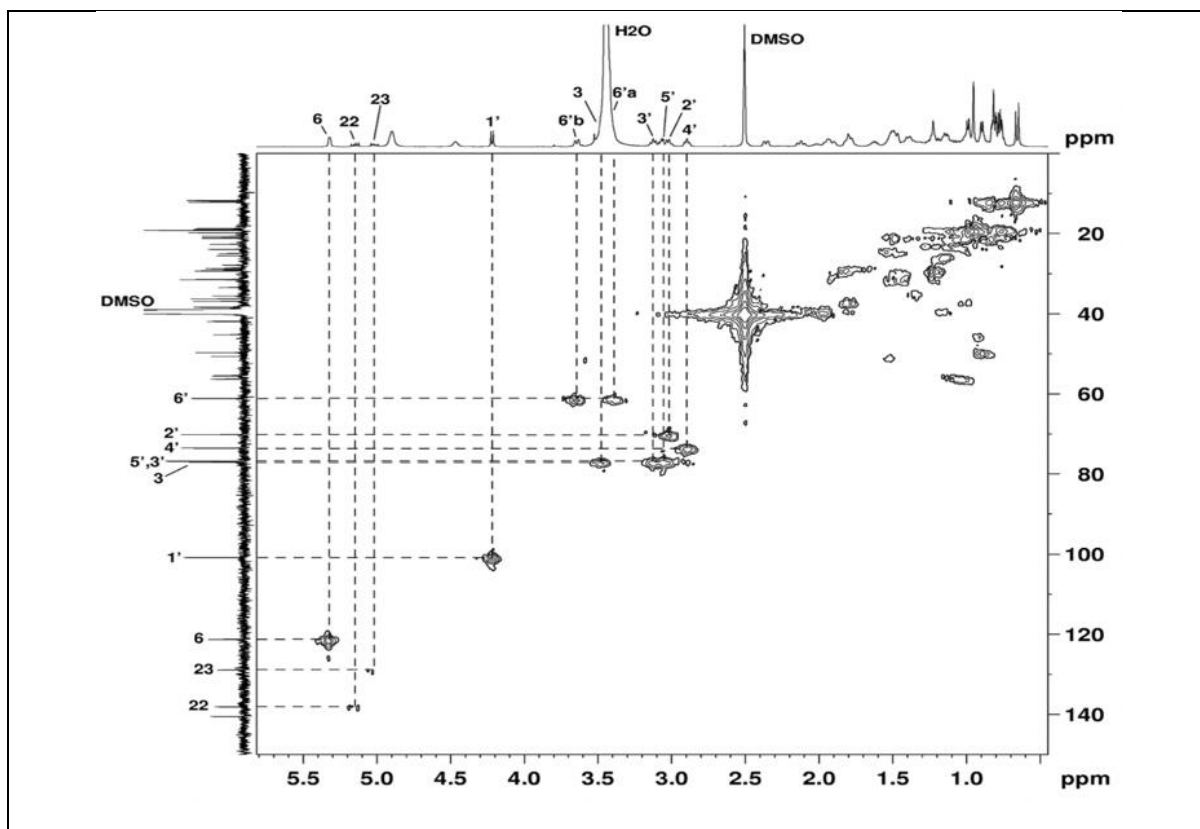


Figure 10. HMQC ( $^1\text{H}$ - $^{13}\text{C}$ ) spectrum of CP-8 (DMSO- $d_6$ )

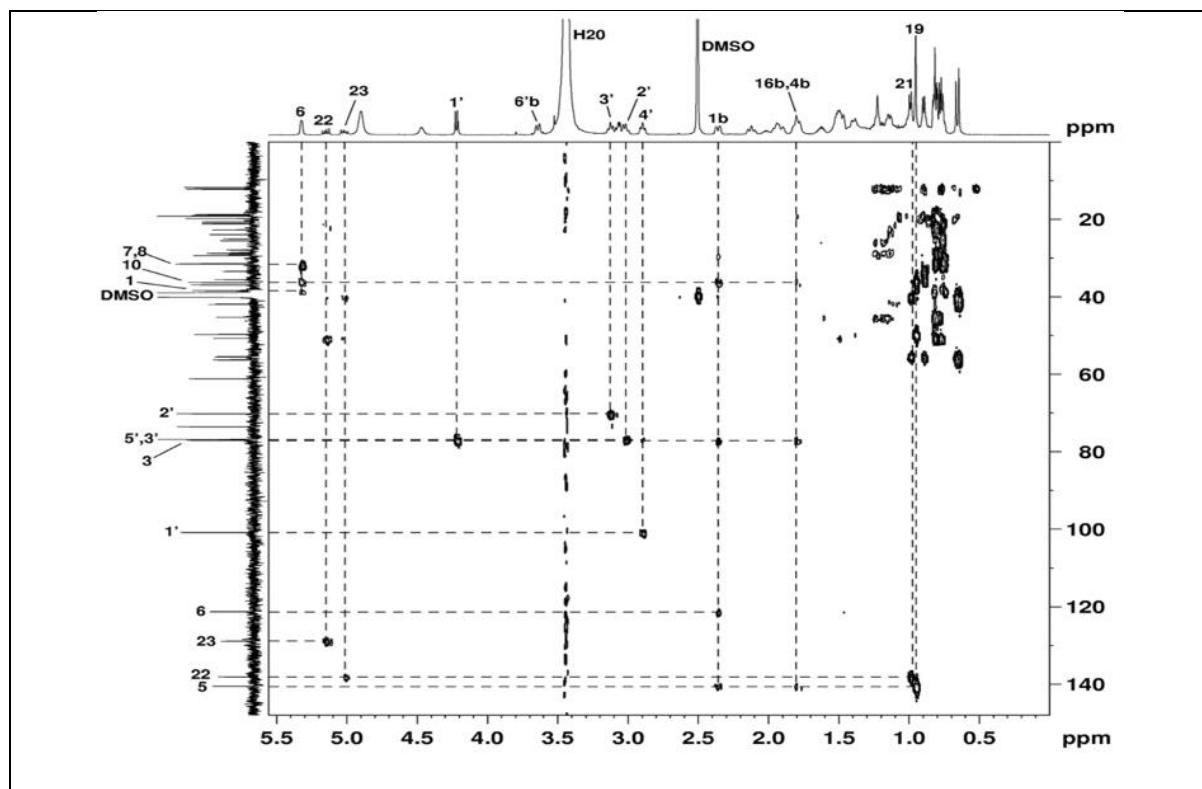


Figure 11. HMBC ( $^1\text{H}$ - $^{13}\text{C}$ ) spectrum of CP-8 (DMSO- $d_6$ )

CP-9 (Figure 12) was isolated from fractions Fma3 to Fma6 by silica gel column chromatography, using hexane and ethyl acetate as eluents. A blue spot corresponding to CP-9 was observed on the TLC plate with the  $R_f$  value of 0.83 (hexane:EtOAc; 9:1 v/v), thus suggesting an acid [41]. Recrystallization of crude CP-9 from methanol gave a white solid (6 mg,  $6.0 \times 10^{-5}$  %) with a melting point of 119-122°C [literature mp: 122-123°C [39]]. The IR spectrum of this compound showed a broad absorption band at  $3363\text{ cm}^{-1}$ , attributed to the O-H stretching of the hydroxyl from an alcohol group. A weak and broad absorption band was observed from  $2500$  to  $3200\text{ cm}^{-1}$ , confirming the acid moiety. An absorption band at  $1670\text{ cm}^{-1}$  was attributed to the C=O stretching of a carboxyl.

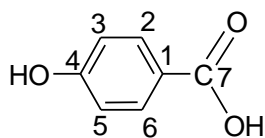


Figure 12. Structure of CP-9 (*p*-hydroxybenzoic acid)

The  $^1\text{H}$ -NMR spectrum of CP-9 indicated the presence of two doublets in the aromatic region of  $\delta_{\text{H}}$  7.97 (d,  $J = 8.7\text{ Hz}$ ) and 6.96 (d,  $J = 8.7\text{ Hz}$ ). Each doublet integrated with two protons, H-2 and H-6 (deshielded), and H-3 and H-5 (less deshielded), respectively. The  $^{13}\text{C}$ -NMR spectrum showed seven

carbon resonances with five signals. The presence of a carboxyl signal resonated in a downfield region at  $\delta_{\text{C}}$  167.48 (C-7). A signal at  $\delta_{\text{C}}$  161.84 was attributed to a hydroxyl bearing carbon, C-4. The experimental NMR data confirmed compound CP-9 was 4-hydroxybenzoic acid or *p*-hydroxybenzoic acid.

CP-10 was isolated from a combination of fractions FM3 to FM5 by silica gel column chromatography, using hexane and ethyl acetate as eluents. A blue spot corresponding to CP-10 was observed on the TLC plate with the  $R_f$  value of 0.31 (hexane:EtOAc; 9:1 v/v). The solvent was removed and a solid was obtained in the form of a white crystal (43 mg,  $4.3 \times 10^{-4}$  %) with a melting point of 62-64°C [literature mp: 63-64°C [36]]. The IR spectrum of this compound displayed absorption bands at 2848 and 2914  $\text{cm}^{-1}$ , attributed to the symmetrical and unsymmetrical stretching of  $\text{C}_{\text{sp}^3}\text{-H}$ . A strong absorption band at 1698  $\text{cm}^{-1}$  was assigned to the C=O stretching of a carboxyl moiety, while a weak absorption band of the O-H stretching of the carboxyl group was observed from 2500 to 3300  $\text{cm}^{-1}$ .

The  $^1\text{H}$ -NMR spectrum of CP-10 indicated a triplet at  $\delta_{\text{H}}$  2.33 for H-2 protons (t,  $J = 7.0\text{ Hz}$ ), which was adjacent to a carbonyl group. Another pair of methylene protons, H-3 gave rise to a multiplet at  $\delta_{\text{H}}$  1.62, while other signals corresponded to other methylene protons. H-4 to H-15 were overlapped and observed as a multiplet at  $\delta_{\text{H}}$  1.22-1.30 ppm. Methyl protons, H-16 appeared as a triplet ( $J = 6.5\text{ Hz}$ ) at  $\delta_{\text{H}}$

0.87 ppm. The  $^{13}\text{C}$ -NMR spectrum showed 16 carbon signals. The most deshielded signal at  $\delta_{\text{C}}$  178.00 was assigned to a carboxyl carbon (C-1), while signals at  $\delta_{\text{C}}$  33.71 and 31.93 corresponded to C-2 and C-14, respectively. Methylene carbons, C-4 to C-13 showed signals in the range of  $\delta_{\text{C}}$  29.07 to 29.70 ppm. The remaining two signals at  $\delta_{\text{C}}$  24.72 and  $\delta_{\text{C}}$  22.70 were assigned to C-3 and C-15, respectively. The signal at  $\delta_{\text{C}}$  14.13 was attributed to a methyl carbon, C-16. Spectral analyses of DEPT experiments indicated that 15 out of 16 carbon atoms in **CP-10** were attached to protons. They comprised of one methyl, 14 methylenes, and one quaternary carbons. Based on the observation, compound **CP-10** was concluded to be palmitic acid, as shown Figure 13.

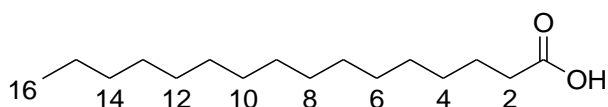


**Figure 13.** Structure of **CP-10** (Palmitic acid)

## 2. Biological Activity Studies of the Extracts of the Leaves of *G. hombroniana* Pierre

Natural antioxidants such as phenols, flavonoids, and tannins are attractive because they can prevent diseases, promote health, and also able to act as anti-aging substances [42]. Antioxidants help to reduce the oxidative damage in humans, which is induced by free radicals and reactive oxygen species under oxidative stress conditions which causes DNA and protein damages, cancer, fast aging, and inflammatory activity [43]. Phenolic compounds are important secondary

metabolites which possess excellent radical scavenging ability. Flavonoids, on the other hand, are a group of polyphenolic compounds with free radical scavenging ability. An easy and sensitive method for the antioxidant screening of plant extracts is DPPH free radical scavenging capacity assay. In the presence of an antioxidant, the DPPH radical will be reduced and the absorbance of the sample decreases [44].

In this work, five different extracts (*n*-hexane, chloroform, ethyl acetate, acetone, and water) were examined for their antioxidant activities using the total phenolic content (TPC), total flavonoid content (TFC), and DPPH antioxidant assays. All these extracts were obtained from 10 kg of fresh leaves of *G. hombroniana* and their yields are tabulated in Table 3.

## 3. Total Phenolic Content (TPC) Assay

Phenolic compounds which possess aromatic rings with one or more hydroxyl groups are the most abundant secondary metabolites present in plants. The attention given to this group of plant metabolites is due to their capacity to scavenge free radicals because of the hydroxyl groups. The choice of the extraction solvents influences the yields of the phenolics being extracted due to the properties of certain plants. The total phenolic contents of different extracts of the leaves of *G. hombroniana* were determined using the Folin-Ciocalteu method, a fast and simple method, with gallic acid as a standard, whereby the phenolic contents can be quantified. A linear calibration curve of gallic acid with  $r^2$  value of 0.992 was obtained.

**Table 3.** Yields of different extracts

Extract	<i>n</i> -hexane	chloroform	Ethyl acetate	acetone	water
Yield (g)	18.0	20.0	14.0	16.0	30.0

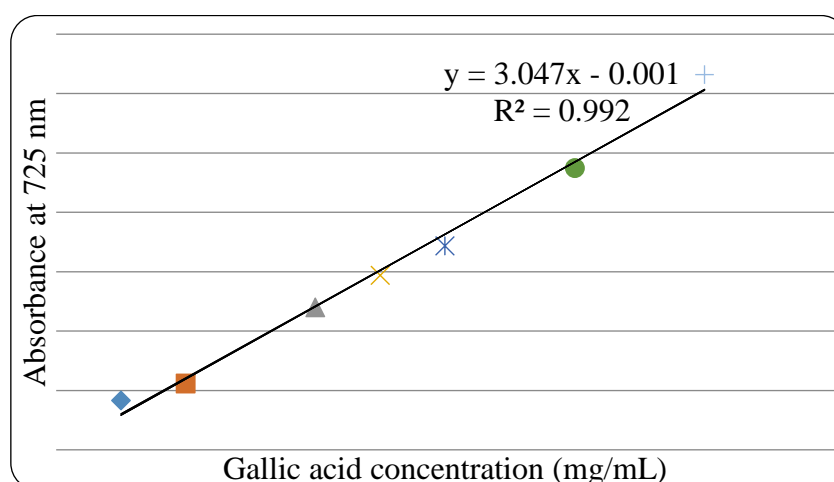


**Figure 14.** Gallic acid calibration curve for TPC assay



**Table 4.** Total phenolic contents of different extracts of the leaves of *G. hombroniana*, expressed as GAE (mg/g)

Extract	Total Phenolic Content
<i>n</i> -hexane	68.05 ± 2.50
Chloroform	150.33 ± 1.69
Ethyl acetate	120.35 ± 4.40
Acetone	98.27 ± 3.70
Water	80.18 ± 1.84

Values are expressed as mean ± SD\* (n=3).

Figure 14 shows the mean TPC of the leaf extracts, which were measured using the equation  $y = 3.047x - 0.001$  ( $R^2 = 0.992$ ), with  $y$  = absorbance at 725 nm and  $x$  = concentration of total phenolic contents in mg mL<sup>-1</sup> of an extract. The total phenolic contents were expressed in term of gallic acid equivalent (GAE) in mg per gram of the fresh weight material. The total phenolic contents (TPC) of different extracts of the leaves of *G. hombroniana* are shown in Table 4.

The chloroform extract showed the highest TPC of 150.33 ± 1.69 mg/g, followed by the ethyl acetate extract of 120.35 ± 4.40 mg/g. Acetone and water extracts showed slightly lower TPC of 98.27 ± 3.70 and 80.18 ± 1.84 mg/g, respectively. The *n*-hexane extract contained the least phenolic compounds, with only 68.05 ± 2.50 mg/g.

Singleton *et al.* reported that the Folin-Ciocalteu reagent oxidized not only the polyphenols but also other substances because phenolic compounds with different number of phenolic -OH groups react differently with the Folin-Ciocalteu reagent [45]. The high value of TPC of the extract is due to the ability of the solvent to dissolve compounds together with the phenolic group. Prior *et al.* also reported that the total phenolic contents in an extract did not refer to a specific polyphenol but also to other compounds which might interfere and react with the reagent [46]. Faujan *et al.* reported that different

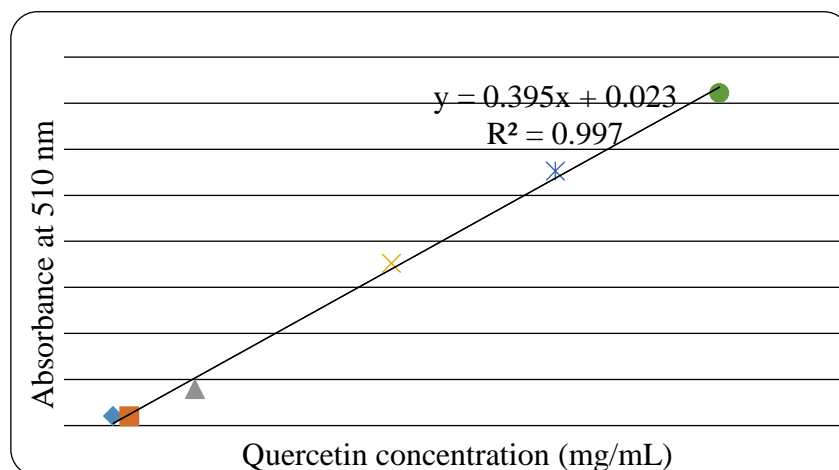
plants, procedures, and standards which were used to express the TPC contributed to the different levels of TPC [47].

#### 4. Total Flavonoid Content (TFC) Assay

In general, flavonoids are large compounds of glycosides with phenolic hydroxyl groups in the ring structure. In this study, the total flavonoid contents of different extracts of the leaves were determined by the aluminium chloride colorimetric assay [48]. In order to quantify the flavonoid contents of the extracts, quercetin was used as the standard in this assay. The TFC was expressed as quercetin equivalent, (QE) in mg/g of an extract.

A linear calibration curve of quercetin with  $r^2$  value of 0.997 was obtained. Figure 15 shows the mean TFC of different leaf extracts measured using the equation of  $y = 0.395x + 0.023$  ( $R^2 = 0.997$ );  $y$  = absorbance at 510 nm and  $x$  = concentration of total flavonoid contents in mg per mL of an extract.

Data in Table 5 show the total flavonoid contents of different extracts of the leaves. The chloroform extract showed the highest TFC value of 85.23 ± 4.13 mg/g, followed by the ethyl acetate and acetone extracts, with TFC values of 79.25 ± 3.17 and 51.32 ± 2.41 mg/g, respectively. The TFC value for the water extract was 44.28 ± 2.10 mg/g, while the *n*-hexane extract has the lowest TFC value of 24.52 ± 1.52 mg/g.

**Figure 15.** Quercetin calibration curve for TFC assay.

**Table 5.** Total flavonoid contents of different extracts from the leaves of *G. hombroniana*, expressed as QE (mg/g)

Extract	Total Flavonoid Content
<i>n</i> -hexane	24.52 ± 1.52
Chloroform	85.23 ± 4.13
Ethyl acetate	79.25 ± 3.17
Acetone	51.32 ± 2.41
Water	44.28 ± 2.10

Values are expressed as mean ± SD\* (n=3).

The TFC results were in a similar manner to those of the TPC results. It was successfully shown that samples with high levels of phenolic contents also contain flavonoids in great amounts [49]. In each solvent extraction, the TPC value was higher than the TFC value, supporting the fact that most flavonoids are phenolic compounds. The basis of total flavonoid assay is when aluminium ions ( $Al^{3+}$ ) form complexes with C-4 keto with either C-3 or C-5 hydroxyl, or with ortho hydroxyl groups in A or B ring [50, 51].

##### 5. Determination of Radical Scavenging Capacity (DPPH) Assay

The DPPH assay is used to determine the radical scavenging capacity of a compound or plant extract, thus the antioxidant potential. DPPH is a stable free

radical (purple) which is reduced to 2,2-diphenyl-1-picrylhydrazine (yellow) by an antioxidant. Antioxidants donate hydrogens from hydroxyl groups to form a stable product, thus interrupting the free radical chain oxidation. A linear calibration curve of Trolox with  $r^2$  value of 0.992 was obtained. Figure 16 shows the mean of DPPH of the leaf extracts measured using the equation of  $y = -0.000x + 0.853$  ( $R^2 = 0.992$ ), where  $y$  = absorbance at 515 nm and  $x$  = concentration of DPPH in  $\mu M$  of an extract.

The concentration of a sample needed to decrease the DPPH concentration by 50% was obtained by interpolation from linear regression analysis and denoted as  $IC_{50}$  value ( $\mu g/mL$ ). All measurements were carried out in triplicates. Trolox was used as the reference compound.

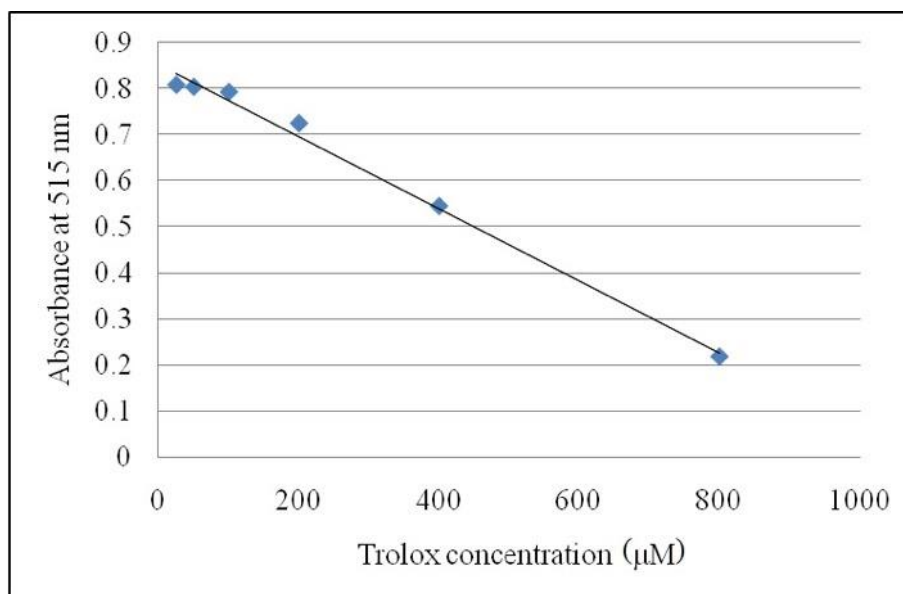


**Figure 16.** Trolox calibration curve for DPPH assay

$$\text{DPPH radical scavenging activity (\%)} = \left[ \frac{(\text{Abs}_{\text{control}} - \text{Abs}_{\text{sample}})}{\text{Abs}_{\text{control}}} \right] \times 100$$

**Table 6.** Percentage inhibition and IC<sub>50</sub> (µg/mL) values of different extracts of the leaves of *G. hombroniana*, using DPPH assay

Extract	% Inhibition	IC <sub>50</sub>
<i>n</i> -hexane	7.54 ± 2.31	3566.55 ± 33.71
Chloroform	55.82 ± 7.89	386.05 ± 19.22
Ethyl acetate	27.58 ± 11.06	415.92 ± 25.74
Acetone	20.54 ± 1.05	478.12 ± 11.23
Water	10.04 ± 8.07	478.52 ± 15.02

Values are expressed as mean ± SD\* (n=3). IC<sub>50</sub> for Trolox positive control for DPPH assay was 9.75 ± 1.29 µg/mL.

**Table 7.** Acetylcholinesterase (AChE) inhibitory activities of different extracts of the leaves of *G. hombroniana*, expressed as percentage inhibition

Extract	% Inhibition
<i>n</i> -hexane	63.44 ± 6.09
Chloroform	54.90 ± 1.89
Ethyl acetate	70.00 ± 1.22
Acetone	72.18 ± 3.27
Water	52.80 ± 3.56

Values are expressed as mean ± SD\* (n=3). % inhibition for physostigmine positive control for AChE inhibition activity was 89.90 ± 0.18.

Data in Table 6 shows the IC<sub>50</sub> (µg/mL) values of different extracts of the leaves of *G. hombroniana*, using the DPPH assay. Almost all the extracts (*n*-hexane, chloroform, ethyl acetate, acetone, and water) showed low percentage of inhibition. Low IC<sub>50</sub> values indicate high radical scavenging capacity [52].

## 6. Cholinesterase Inhibitory Studies

Alzheimer's Disease or AD is a neurodegenerative disorder caused by the death of nerve cells known as cholinergic neurons, which are responsible for the storage and process of information in a human brain [53]. One of the contributing factors of this disease is an elevated level of acetylcholinesterase (AChE). This enzyme is responsible for the termination of nerve impulse transmission, thus leading to dementia [54]. In order to restore the level of acetylcholine in the brain, many researches have been conducted to search for new AChE inhibitors. However, only a few AChE inhibitors have been approved for treatment due to the side effects of synthetic drugs [55].

The five different extracts from the leaves of *G. hombroniana* were assayed for their AChE inhibitory activities. The percentage of inhibition of each extract is reported in Table 7.

All extracts showed weak inhibition. Among the five extracts, the acetone extract showed the highest percentage of inhibition of 72.18 ± 3.27 %. Chloroform, *n*-hexane, and ethyl acetate extracts showed 55-70% of inhibition against AChE. The water extract showed the lowest percentage of inhibition of 52.80 ± 3.56 %.

## CONCLUSION

The phytochemical investigation of the leaf extracts of *G. hombroniana* has led to the isolation of ten known compounds from the chloroform extract, which included friedelin (CP-1), stigmasterol (CP-2), taraxerol (CP-3), garcihombrone D (CP-4), lupeol (CP-5), betulin (CP-6), betulinic acid (CP-7), stigmasterol glucoside (CP-8), and two acids, namely *p*-hydroxybenzoic acid (CP-9) and palmitic acid (CP-10). The elucidation of the structures of all the compounds was done using FT-IR and NMR spectroscopic analyses, together with EI mass spectrometry. Different extracts (*n*-hexane, chloroform, ethyl acetate, acetone, and water extracts) of the leaves of *G. hombroniana* were tested for their antioxidant activities. The total phenolic content (TPC), total flavonoid content (TFC) and DPPH assays for all the extracts showed weak antioxidant activities. For anti-Alzheimer's (cholinesterase) activity, all extracts showed weak inhibition of 50-75% inhibition against AChE. Even though the evaluation of phytochemicals and biological activities was weak in these studies, the information regarding on the prospective use of medicinal plants as sources of new drugs can be used with some modifications for future work.

## ACKNOWLEDGEMENT

The authors would like to thank Universiti Sains Malaysia (USM) in providing the lab facilities and Universiti Malaysia Sabah (UMS).

## REFERENCES

1. Ruma, K., Sunil, K., Prakash, H. S. (2013) Antioxidant, Anti-inflammatory, Antimicrobial and Cytotoxic Properties of Fungal Endophytes from *Garcinia* Species. *International Journal of Pharmacy and Pharmaceutical Sciences*, **5**(3), 889–897.
2. Nazre, M. (2010) Historical review and notes on the correct scientific name for seashore mangosteen. *Genetic Resources and Crop Evolution*, **57**(8), 1249–1259.
3. Miliken, W. (1994) Ethnobotany of the Yali of West Papua, Royal Botanic Garden, Edinburgh, UK.
4. Ogu, E. O., Agu, R. C. (1995) A comparison of some chemical properties of *Garcinia kola* and hops for assessment of *Garcinia* brewing value. *Bioresource Technology*, **54**(1), 1–4.
5. Negi, P. S., Jayaprakasha, G. K., Jena, B. S. (2008) Antibacterial activity of the extracts from the fruit rinds of *Garcinia cowa* and *Garcinia pedunculata* against food borne pathogens and spoilage bacteria. *LWT - Food Science and Technology*, **41**(10), 1857–1861.
6. Mackeen, M.M.; Ali, A.M.; Lajis, N.H.; Kawazu, K.; Hassan, Z.; Amran, M.; Habsah, M.; Mooi, L.Y.; Mohamed, S.M. (2000). Antimicrobial, antioxidant, antitumour-promoting and cytotoxic activities of different plant part extracts of *Garcinia atroviridis* Griff. ex T. Anders. *Journal of Ethnopharmacology*, **72**(3), 395–402.
7. Mackeen, M. M., Ali, A. M., Lajis, N. H., Kawazu, K., Kikuzaki, H., Nakatani, N. (2002) Antifungal garcinia acid esters from the fruits of *Garcinia atroviridis*. *Zeitschrift fur Naturforschung - Section C Journal of Biosciences*, **57**(3-4), 291–295.
8. Mahabusarakam, W., Wiriyaচিত্রা, P., Taylor, W. C. (1987) Chemical Constituents of *Garcinia mangostana*. *Journal of Natural Products*, **50**(3), 474–478.
9. Hemshekhar, M., Sunitha, K., Santhosh, M. S., Devaraja, S., Kemparaju, K., Vishwanath, B. S., Niranjana, S. R., Girish, K. S. (2011) An overview on genus *Garcinia*: phytochemical and therapeutical aspects. *Phytochemistry Reviews*, **10**(3), 325–351.
10. Elya, B., Katrin, Mun'im, A., Hasiholan, A., Marlin, I., Mailandari, M. (2012) Antioxidant Activities of Leaves Extracts of Three Species of *Garcinia*. *International Journal of Medicinal and Aromatic Plants*, **2**(4), 691–693.
11. Subhashini, N., Nagarajan, G., Kavimani, S. (2011) *In vitro* Antioxidant and Anticholinesterase Activities of *Garcinia Combogia*. *International Journal of Pharmacy and Pharmaceutical Sciences*, **3**(3), 129–132.
12. Wu, J. H., Tung, Y. T., Chyu, C. F.; Chien, S. C., Wang, S. Y., Chang, S. T., Kuo, Y. S. (2008) Antioxidant Activity and Constituents of Extracts from the Root of *Garcinia multiflora*. *Journal of Wood Science*, **54**, 383–389.
13. Jamila, N., Khairuddean, M., Lai, C. S., Osman, H., Yaacob, N. S., Murugaiyah, V., Khaw, K. Y. (2013) Antioxidant, Anti-cholinesterase and Antibacterial Activities of the Bark Extracts of *Garcinia hombroniana*. *African Journal of Pharmacy and Pharmacology*, **7**(8), 454–459.
14. Jamila, N., Khan, N., Khan, A. A., Khan, I., Khan, S. N., Zakariae, Z. A., Khairuddean, M., Osman, H., Kim, K. S. (2017) *In vivo* carbon tetrachloride-induced hepatoprotective and *in vitro* cytotoxic activities of *Garcinia hombroniana* (seashore mangosteen). *African Journal of Traditional, Complementary and Alternative Medicines*, **14**(2), 374–382.
15. Muhammad, N. A., Basar, N., Jamil, S. (2019) Antibacterial Activity of Phytochemicals from *Garcinia parvifolia* Miq. and *Garcinia hombroniana* Pierre. *Journal of Science and Mathematics Letters*, **7**, 44–51.
16. Kamal, Z., Ullah, F., Ayaz, M., Sadiq, A., Ahmad, S., Zeb, A., Hussain, A., Imran, M. (2015) Anticholinesterase and Antioxidant Investigations of Crude Extracts, Subsequent Fractions, Saponins and Flavonoids of *Atriplex laciniata* L.: Potential Effectiveness in Alzheimer's and other Neurological Disorders. *Biological Research*, **48**(21), 2–11.
17. Hlila, M. B., Mosbah, H., Mssada, K., Jannet, H. B., Aouni, M., Selmi, B. (2015) Acetylcholinesterase Inhibitory and Antioxidant Properties of Roots Extracts from the Tunisian *Scabiosa arenaria* Forssk. *Industrial Crops and Products*, **67**, 62–69.
18. Rukachaisirikul, V., Saelim, S., Karnsomchoke, P., Phongpaichit, S. (2005) Friedolanostanes and Lanostanes from the Leaves of *Garcinia hombroniana*. *Journal of Natural Products*, **68**(8), 1222–1225.

19. Jamain, Z., Khairuddean, M., Guan-Seng, T. (2020) Synthesis of new star-shaped liquid crystalline cyclotriphosphazene derivatives with fire retardancy bearing amide-azo and azo-azo linking units, *Int. J. Mol. Sci.*, **21**, 4267.
20. Brand-Williams, W., Cuvelier, M. E., Berset, C. (1995) Use of free radical method to evaluate antioxidant activity. *LebensmWiss Technology*, **28**, 25–30.
21. Ellman G. L., Courtney K. D., Andres V. Jr., Featherstone R. M. (1961) A new and rapid colorimetric determination of acetylcholinesterase activity, *Biochem. Pharmacol.*, **7**, 88–95.
22. Ahmed, T., Gilani, A. H. (2009) Inhibitory effect of curcuminoids on acetylcholinesterase activity and attenuation of scopolamine-induced amnesia may explain medical use of turmeric in Alzheimer's disease, *Biochemical Pharmacology*, **91**, 554–559.
23. Obregon, L. M., Taylor, M. F., Mir, G., Pereyra, C. A., Pianzola, H., Petrone, H., Baran, M., Menna M. E. (2005) Parathyroidectomy for Parathyroid Carcinoma in Renal Transplantation, *Transplantation Proceedings*, **37**, 973–976.
24. Mann, A., Ibrahim, K., Oyewale, A. O., Amupitan, J. O., Fatope, M. O.; Okugun, J. I. (2011) Antimycobacterial Friedelane-terpenoid from the Root Bark of *Terminalia Avicennioides*. *American Journal of Chemistry*, **1**(2), 52–55.
25. Mawa, S., Said, I. M. (2012) Chemical Constituents of *Garcinia prainiana*. *Sains Malaysiana*, **41**(5), 585–590.
26. Pierre, L. L., Moses, M. N. (2015) Isolation and Characterisation of Stigmasterol and  $\beta$ -Sitosterol from *Odontonema strictum* (Acanthaceae). *Journal of Innovations in Pharmaceuticals and Biological Sciences*, **2**(1), 88–95.
27. Kamboj, A., Saluja, A. K. (2011) Isolation of Stigmasterol and  $\beta$ -Sitosterol from Petroleum Ether Extract of Aerial Parts of *Ageratum conyzoides* (Asteraceae). *International Journal of Pharmacy and Pharmaceutical Sciences*, **3**(1), 94–96.
28. Forgo, P., Kövér, K. E. (2004) Gradient enhanced selective experiments in the  $^1\text{H}$  NMR chemical shift assignment of the skeleton and side-chain resonances of stigmasterol, a phytosterol derivative. *Steroids*, **69**, 43–50.
29. Shyamkumar, Ishwar, B. (2012) Anti Inflammatory, Analgesic and Phytochemical Studies of *Clitoria ternatea* Linn Flower Extract. *International Research Journal of Pharmacy*, **3**(3), 208–210.
30. Swain, S. S., Rout, K. K., Chand, P. K. (2012) Production of Triterpenoid Anti-cancer Compound Taraxerol in Agrobacterium-Transformed Root Cultures of Butterfly Pea (*Clitoria ternatea* L.). *Applied Biochemistry and Biotechnology*, **168**(3), 487–503.
31. Klaiklay, S. (2009) Chemical Constituents from the Twigs of *Garcinia hombroniana*, the Leaves of *Garcinia prainiana* and the Roots of *Clerodendrum petasites* S. Moore. Thesis ([http://opus.bath.ac.uk/39800/1/Accepted\\_version.pdf](http://opus.bath.ac.uk/39800/1/Accepted_version.pdf) - Accessed date: Feb 2014).
32. Rukachaisirikul, V., Adair, A., Dampawan, P., Taylor, W. C., Turner, P. T. (2000) Lanostanes and friedolanostanes from the pericarp of *Garcinia hombroniana*. *Phytochemistry*, **55**(2), 183–188.
33. Manjula, K., Phazanichamy, K., Kumaran, S., Eevera, T., Keefe, C. D., Rajendran, K. (2012) Growth Characterization of Calcium Oxalate Monohydrate Crystals Influenced by *Costus igneus* Aqueous Stem Extract. *International Journal of Pharmacy and Pharmaceutical Sciences*, **4**(1), 261–270.
34. Badria, F. A., Botros, R. M., Galal, T. M., Amer, M. M. A., Naturforsch, Z. (2003) Immunomodulatory Triterpenoids from the Oleogum Resin of *Boswellia carterii* Birdwood, *PubMed Journals*, **58c**, 505–516.
35. Raza, R., Ilyas, Z., Ali, S., Nisar, M., Khokhar, M. Y., Iqbal, J. (2015) Identification of Highly Potent and Selective  $\alpha$ -Glucosidase Inhibitors with Antiglycation Potential, Isolated from *Rhododendron arboreum*. *Records of Natural Products*, **9**(2), 262–266.
36. Joshi, H., Saxena, G. K., Singh, V., Arya, E., Singh, R. P. (2013) Phytochemical Investigation, Isolation and Characterization of Betulin from Bark of *Betula utilis*. *Journal of Pharmacognosy and Phytochemistry*, **2**(1), 145–151.
37. Prakash, C. V. S., Prakash, I. (2012) Isolation and Structural Characterization of Lupane Triterpenes from *Polypodium Vulgare*. *Research Journal of Pharmaceutical Sciences*, **1**(1), 23–27.
38. Rai, N. P., Adhikari, B. B., Paudel, A., Masuda, K., Mckelvey, R. D., Manandhar, M. D. (2006)

- Phytochemical Constituents of the Flowers of *Sarcococca coriacea* of Nepalese origin. *Journal of Nepal Chemical Society*, **21**, 1–7.
39. Falodun, A., Ali, S., Quadir, I. M., Choudhary, I. M. I. (2008) Phytochemical and biological investigation of chloroform and ethylacetate fractions of *Euphorbia heterophylla* leaf (Euphorbiaceae). *Journal of Medicina IPlants Research*, **2**(12), 365–369.
40. Ridhay, A., Noor, A., Soekamto, N. H., Harlim, T., Altena, I. V. (2012) A stigmasterol glycoside from the root wood of *Melochia umbellata* (Houtt) Stapf var. *degrabrata* K. *Indonesian Journal of Chemistry*, **12**(1), 100–103.
41. Yayli, N., Yildirim, N., Usta, A., Ozkurt, S., Akgun, V. (2003) Chemical Constituents of *Campanula lactiflora*. *Turkish Journal of Chemistry*, **27**, 749–755.
42. Saxena, M., Saxena, J. (2013) Correlation of TPC and TFC with Antioxidant Activity of Selected Indian Medicinal Plants. *American Journal of Pharmtech Research*, **3**(2), 233–241.
43. Blois, M. S. (1958) Antioxidant determinations by the use of a stable free radical. *Nature*, **181**, 1199–1200.
44. Gulcin, I., Huyut, Z., Elmastas, M., Aboul-Enein, H. Y. (2010) Radical Scavenging and Antioxidant Activity of Tannic Acid. *Arabian Journal of Chemistry*, **3**(1), 43–53.
45. Singleton, V. L., Orthofer, R. M., Ramuela-Raventos, R. M. (1999) Analysis of total phenols and antioxidants and other substrates by means of Folin–Ciocalteu reagent. *Methods Enzymology*, **299**, 152–178.
46. Prior, R. L., Wu, X. L., Schaich, K. (2005) Standardized methods for the determination of antioxidant capacity and phenolics in foods and dietary supplements. *Journal of Agricultural and Food Chemistry*, **53**(10), 4290–4302.
47. Faujan, N. H., Abdullah, N., Sani, N. A., Babji, A. S. (2007) Antioxidative activities of water extracts of some Malaysian herbs. *ASEAN Food Journal*, **14**(1), 61–68.
48. Cao, G., Sofic, E., Prior, R. L. (1997) Antioxidant and prooxidant behavior of flavonoids: structure–activity relationships. *Free Radical Biology and Medicine*, **22**, 749–760.
49. Esmaeili, A. K., Taha, R. M., Mohajer, S., Banisalam, B. (2015) Antioxidant Activity and Total Phenolic and Flavonoid Content of Various Solvent Extracts from *In Vivo* and *In Vitro* Grown *Trifolium pratense* L. (Red Clover). *Biomed Research International*, **2015**, 1–11.
50. Ahmed, D., Khan, M. M., Saeed, R. (2015) Comparative Analysis of Phenolics, Flavonoids, and Antioxidant and Antibacterial Potential of Methanolic, Hexanic and Aqueous Extracts from *Adiantum caudatum* Leaves. *Antioxidants*, **4**, 349–409.
51. Amic, D., Amic, D. D., Beslo, D., Rastija, V., Lucic, B., Trinajtic, N. (2007) SAR and QSAR of the Antioxidant Activity of Flavonoids. *Current Medicinal Chemistry*, **14**, 827–845.
52. Fidrianny, I., Rahmiyani, I., Wirasutisna, K. R. (2013) Antioxidant Capacities from Various Leaves Extracts of Four Varieties Mangoes Using DDPH, ABTS Assays and Correlation with Total Phenolic, Flavonoid, Carotenoid. *International Journal of Pharmacy and Pharmaceutical Sciences*, **5**(4), 189–194.
53. Vladimir-Knezevic, S., Blazekovic, B., Kindl, M., Vlastic, J., Lower-Nedza, A. D., Brantner A. H. (2014) Acetylcholinesterase Inhibitory, Antioxidant and Phytochemical Properties of Selected Medicinal Plants of the Lamiaceae Family. *Molecules*, **19**, 767–782.
54. Ali-Hassan, S. H., Fry, J. R., Abu-Bakar, M. F. (2013) Antioxidative Phytochemicals and Anti-Cholinesterase Activity of Native Kembayau (*Canarium odontophyllum*) Fruit of Sabah, Malaysian Borneo. *Journal of Nutrition and Food Sciences*, **4**(1), 1–6.
55. Yang, Z., Zhang, X., Duan, D., Song, Z., Yang, M., Li, S. (2009) Modified TLC bioautographic method for screening acetylcholinesterase inhibitors from plant extracts. *Journal of Separation Science*, **32**, 3257–3259.